

Mechanisms of *Trichodesmium* demise within the New Caledonian lagoon during the VAHINE mesocosm experiment

D. Spungin¹, U. Pfreundt², H. Berthelot³, S. Bonnet^{3,4}, D. AlRoumi⁵, F. Natale⁵, W.R. Hess², K.D. Bidle⁵, I. Berman-Frank¹

[1] {The Mina and Everard Goodman Faculty of Life Sciences, Bar-Ilan University, Ramat-Gan, Israel}

[2] {University of Freiburg, Faculty of Biology, Schänzlestr. 1, D-79104 Freiburg, Germany}

[3] {Aix Marseille Université, CNRS/INSU, Université de Toulon, IRD, Mediterranean Institute of Oceanography (MIO) UM 110, 13288, Marseille, France}

[4] {Institut de Recherche pour le Développement (IRD), AMU/CNRS/INSU, Université de Toulon, Mediterranean Institute of Oceanography (MIO) UM 110, 13288, Marseille-Noumea, France-New Caledonia}

[5] {Department of Marine and Coastal Sciences, Rutgers University, New Brunswick, NJ, USA}

Correspondence to: I. Berman-Frank (ilana.berman-frank@biu.ac.il)

Abstract

The globally important marine diazotrophic cyanobacterium *Trichodesmium* is abundant in the New Caledonian lagoon (Southwestern Pacific ocean) during austral spring/summer. We investigated the cellular processes mediating *Trichodesmium* mortality from large surface accumulations (blooms) in the lagoon. *Trichodesmium* cells (and associated microbiota) were collected at the time of surface accumulation, enclosed under simulated ambient conditions, and sampled over time to elucidate the stressors and subcellular underpinning of rapid biomass demise (> 90 % biomass crashed within ~ 24 h). Metatranscriptomic profiling of *Trichodesmium* biomass, 8 h and 22 h after incubations of surface accumulations, demonstrated upregulated expression of genes required to increase phosphorus (P) and iron (Fe) availability and transport while genes responsible for nutrient storage were downregulated. Total viral abundance, oscillated throughout the experiment and showed no significant relationship with the development or demise of the *Trichodesmium* biomass. Enhanced caspase-specific activity and upregulated expression of a suite of metacaspase genes, as the *Trichodesmium* biomass crashed, implicated autocatalytic programmed cell death (PCD) as the mechanistic cause. Concurrently, genes associated with buoyancy and gas-vesicle production were strongly downregulated concomitant with increased production and high concentrations of transparent exopolymeric particles (TEP). The rapid, PCD-mediated, decline of the *Trichodesmium* biomass, as we observed from our incubations, parallels mortality rates reported from *Trichodesmium* blooms *in situ*. Our results suggest that, whatever the ultimate factor, PCD-mediated death in *Trichodesmium* can rapidly terminate blooms, facilitate aggregation, and expedite vertical flux to depth.

1 Introduction

The filamentous N₂-fixing (diazotrophic) cyanobacteria *Trichodesmium* spp. are important contributors to marine N₂ fixation as they form massive blooms (surface accumulations with high biomass density) throughout the oligotrophic marine sub-tropical and tropical oceans (Capone et al., 2004; Capone and Carpenter, 1982; Capone et al., 1997). These surface blooms with densities of 3000 to > 10,000 trichomes L⁻¹ and chlorophyll *a* (Chl *a*) concentrations ranging from 1-5 mg L⁻¹ develop swiftly and are characterized by high rates of CO₂ and N₂ fixation (Capone et al., 1998; Luo et al., 2012; Rodier and Le Borgne, 2008; Rodier and Le Borgne, 2010). *Trichodesmium* blooms also occur frequently during austral summer between November and March over large areas of the New Caledonian lagoon in the Southwest Pacific Ocean (Dandonneau and Gohin, 1984; Dupouy et al., 2011).

Trichodesmium has been extensively investigated [reviewed in Capone et al. (1997); and Bergman et al. (2012)]. Yet, relatively few publications have examined the mortality and fate of these blooms that often collapse abruptly with mortality rates paralleling growth rates and biomass declines > 50 % occurring within 24 h from peak abundance (Bergman et al., 2012; Rodier and Le Borgne, 2008; Rodier and Le Borgne, 2010). Cell mortality can occur due to grazing of *Trichodesmium* by pelagic harpacticoid copepods (O'Neil, 1998) or by viral lysis (Hewson et al., 2004; Ohki, 1999). Both iron (Fe) and phosphorus (P) availability regulate N₂ fixation and production of *Trichodesmium* populations, causing a variety of stress responses when these nutrients are limited (Berman-Frank et al., 2001). Fe depletion as well as oxidative stress can also induce in *Trichodesmium* a genetically controlled programmed cell death (PCD) that occurs in both laboratory cultures and in natural populations (Bar-Zeev et al., 2013; Berman-Frank et al., 2004; Berman-Frank et al., 2007). Mortality of *Trichodesmium* via PCD is morphologically and physiologically distinct from necrotic death and triggers rapid sinking of biomass that could enhance carbon export in oligotrophic environments (Bar-Zeev et al., 2013). Sinking is due to concomitant internal cellular degradation, vacuole loss, and the increased production of extracellular polysaccharide aggregates, operationally defined as transparent exopolymeric particles (TEP) (Bar-Zeev et al., 2013; Berman-Frank et al., 2004; Berman-Frank et al., 2007).

The VAHINE project investigated the fate of newly fixed N by diazotrophs and aimed to test changes in organic matter export, following diazotroph development and mortality. For this, large (50 m³) mesocosms were deployed in the New Caledonian lagoon and followed over the course of 23 days (Bonnet et al., 2016a). Our objective during the VAHINE project

was to study the involvement of PCD in the fate of natural *Trichodesmium* blooms induced in these mesocosms. While *Trichodesmium* was initially present, and conditions in the mesocosms appeared favorable, no *Trichodesmium* blooms developed within the mesocosms, yet UCYN-C did increase, allowing to meet the scientific objectives of the project (Berthelot et al., 2015; Bonnet et al., 2016a; Turk-Kubo et al., 2015). However, *Trichodesmium* developed at different phases of the experimental period outside the mesocosms (Turk-Kubo et al., 2015). Here, we investigated mortality processes in a short-lived *Trichodesmium* bloom that developed and crashed in the lagoon waters at the end of the VAHINE experiment. Using a series of microcosm incubations with collected *Trichodesmium* biomass, we elucidated the stressors and subcellular underpinning of rapid (~ 24 h) biomass demise and disappearance. Here we present, for the first time, physiological, biochemical, and metatranscriptomic evidence for nutrient-stress induced PCD in natural populations that lead to *Trichodesmium* mortality including concomitant downregulation of gas vesicle synthesis and enhanced TEP production. Such mechanisms would lead to enhanced export flux in natural blooms that also crash within 1-2 days.

2 Methods

2.1. Sampling site and sampling conditions during pre-bloom periods

Our study was performed during the VAHINE mesocosm project set 28 km off the coast of New Caledonia from 13 January 2013 (day 1) to 6 February 2013 in the New Caledonian oligotrophic lagoon (22°29.10' S, 166° 26.90' E). The 25 m deep sandy-bottom lagoon is generally protected from the dominant trade winds yet the waters of the lagoon are influenced by the oligotrophic oceanic waters coming into the lagoon via the Boulari Pass (Bonnet et al., 2016a). Detailed descriptions of the site selection and sampling strategy are provided elsewhere (Bonnet et al., 2016a). The lagoon water outside the mesocosms was sampled daily during the experiment and serve as 'pre-bloom' data. Large volume samples (50 L) were collected from 1, 6, and 12 m depths at 07:00 using a Teflon® PFA pump and PVC tubing. Samples were immediately transferred back to laboratories aboard the R/V Alis and subsampled for a suite of parameters [as described below and in Bonnet et al. (2016a)]. On day 23 at 12:00 h, we observed a large surface accumulation of *Trichodesmium* in the lagoon close to the enclosed mesocosms. This biomass accumulation (hereafter called – “bloom”) served as the source for experiments 1 and 2 to examine the fate of *Trichodesmium* (section 2.2, Fig. S1).

120

121 **2.2. Short-term incubations to assess bloom decline**

122 **Experiment 1** – *Trichodesmium* filaments and colonies were collected from the dense surface
123 bloom (day 23, 12:00 h; designated T₀, Fig. 2a-c) using a plankton net (mesh size, 80 µm)
124 towed through different patches of the bloom from the surface water. The total contents of the
125 net were combined and resuspended in filtered seawater (FSW) (0.2 µm pore size), split
126 between six identical 4.5 L Nalgene polycarbonate bottles (Fig. 2d-e), and incubated as
127 detailed below. Based on previous experience (Berman-Frank et al., 2004), resuspension of
128 *Trichodesmium* cells in the extremely high densities of the surface blooms (> 1 mg L⁻¹ Chl *a*;
129 Fig. 2a-c) would cause an almost immediate crash of the biomass. Consequently, we
130 resuspended the collected biomass in FSW at ~ 1000 fold lower cell densities (150 µg L⁻¹) that
131 resemble the cellular abundance at the edges of the slicks (Fig. 2). **Experiment 2** – Seawater
132 from the surface bloom was collected 5 h after the initial surface bloom was sighted (day 23,
133 17:00) by using a Teflon® PFA pump and PVC tubing directly filling nine 20 L polyethylene
134 carboys gently to avoid destroying biomass. Bottles from experiments 1 and 2 were placed in
135 on-deck incubators, filled with running seawater to maintain ambient surface temperature (~
136 26 °C), and covered with neutral screening at 50 % surface irradiance levels. Water from
137 experiment 1 was sampled every 2-4 h until the biomass collapsed (after ~ 22 h) for: Chl *a*
138 concentration, caspase activity, 16S rRNA gene sequencing, and metatranscriptomics. Water
139 from experiment 2 was sampled for PON, POC, NH₄⁺, N₂ fixation rates, TEP production, and
140 virus abundance (days 23-25) (Fig. S1). Prior to incubations, all incubation bottles and
141 carboys were washed with 10 % HCl overnight and rinsed 3 times with ambient seawater.

142 **2.3. Chlorophyll *a* concentrations**

143 Samples for the determination of Chl *a* concentrations during pre-bloom days were collected
144 by filtering 550 mL of seawater on GF/F filters. Filters were directly stored in liquid nitrogen.
145 Chl *a* was extracted in methanol and measured fluorometrically (Herbland et al., 1985).
146 During short-term experiment 1, samples for Chl *a* were collected by filtering 200 mL on
147 GF/F filters (Whatman, Kent, UK). Chl *a* was extracted in methanol and measured
148 spectrophotometrically (664 and 750 nm; CARY100, Varian, Santa Clara, CA, USA)
149 according to Tandeau de Marsac and Houmard (1988).

150

151

152 **2.4. Particulate organic carbon (POC) and nitrogen (PON)**

153 Detailed POC and PON analyses are described in Berthelot et al. (2015). POC samples were
154 collected by filtering 2.3 L of seawater through pre-combusted (450 °C, 4 h) GF/F filter and
155 determined using the combustion method (Strickland and Parsons, 1972) on an EA 2400 CHN
156 analyzer. Samples for PON concentrations were collected by filtering 1.2 L of water on pre-
157 combusted (450 °C, 4 h) and acid washed (HCl, 10 %) GF/F filters and analyzed according to
158 the wet oxidation protocol described in Pujo-Pay and Raimbault (1994) with a precision of
159 0.06 $\mu\text{mol L}^{-1}$.

160 **2.5. N₂ fixation rates and NH₄⁺ concentrations**

161 N₂-fixation rate measurements used in experiment 2 are described in detail in (Berthelot et al.,
162 2015). Samples were collected at 17:00 in 4.5 L polycarbonate bottles and amended with ¹⁵N₂-
163 enriched seawater, within an hour of biomass collection, according to the protocol developed
164 by Mohr et al. (2010) and Rahav et al. (2013). Briefly, seawater was degassed through a
165 degassing membrane (Membrana, Minimodule®, flow rate fixed at 450 mL min⁻¹) connected
166 to a vacuum pump. Degassed seawater was amended with 1 mL of ¹⁵N₂ (98.9 % atom ¹⁵N,
167 Cambridge Isotopes) per 100 mL. The bottle was shaken vigorously and incubated overnight
168 at 3 bars to promote ¹⁵N₂ dissolution. Incubation bottles were amended with 1:20 (vol:vol) of
169 ¹⁵N₂-enriched seawater, closed without headspace with silicone septum caps, and incubated
170 for 24 h under *in situ*-simulated conditions in on-deck incubators (described above). 2.2 L
171 from each experimental bottle was filtered under low vacuum pressure (< 100 mm Hg) onto a
172 pre-combusted (450 °C, 4 h) GF/F filter (25 mm diameter, 0.7 μm nominal porosity). The
173 filters were stored at -20 °C and dried for 24 h at 60 °C before mass spectrometric analysis.
174 PON content and PON ¹⁵N enrichments were determined using a Delta plus Thermo Fisher
175 Scientific isotope ratio mass spectrometer (Bremen, Germany) coupled with an elemental
176 analyzer (Flash EA, Thermo Fisher Scientific). N₂-fixation rates were calculated according to
177 the equations detailed in Montoya et al. (1996). We assumed significant rates when the ¹⁵N
178 enrichment of the PON was higher than three times the standard deviation obtained from T₀
179 samples. The ¹⁵N batch did not indicate that our results were overestimated by contamination
180 of the spike solution (Berthelot et al. 2015).
181 Samples for NH₄⁺ were collected in 40 mL glass vials and analyzed by the fluorescence
182 method according to Holmes et al. (1999), using a Trilogy fluorometer (Turner Design).

2.6. Transparent exopolymeric particles (TEP)

Water samples (100 mL) were gently (< 150 mbar) filtered through 0.45 µm polycarbonate filter (GE Water & Process Technologies). Filters were then stained with a solution of 0.02 % Alcian blue (AB), 0.06 % acetic acid (pH of 2.5), and the excess dye was removed by a quick deionized water rinse. Filters were then immersed in sulfuric acid (80 %) for 2 h, and the absorbance (787 nm) was measured spectrophotometrically (CARY 100, Varian). AB was calibrated using a purified polysaccharide gum xanthan (GX) (Passow and Alldredge, 1995). TEP concentrations (µg GX equivalents L⁻¹) were measured according to (Passow and Alldredge, 1995).

2.7. Virus abundance

Total seawater (1 mL) was fixed with 0.5 % glutaraldehyde and snap frozen in liquid N₂ until processed. Flow cytometry was conducted using an Influx Model 209S Mariner flow cytometer and high-speed cell sorter equipped with a 488 nm 200 mW blue laser, 4 way sort module, 2 scatter, 2 polarized and 4 fluorescence detectors (BD Biosciences). Viral abundance was determined by staining fixed seawater samples with SYBR Gold (Life Technologies) and measurements of green fluorescence (520 nm, 40 nm band pass). Samples were thawed, diluted 25-fold in 0.22 µm-filtered Tris/EDTA (TE) buffer (pH 8), stained with SYBR Gold (0.5 - 1X final concentration), incubated for 10 min at 80°C in the dark, cooled to RT for 5 min, and mixed thoroughly by vortexing prior to counting on the Influx (Brussaard, 2003). Viral abundance was analyzed using a pressure differential (between sheath and sample fluid) of 0.7, resulting in a low flow rate for higher event rates of virus like particles counts.

2.8. Caspase activity

Biomass was collected on 25 mm, 5 µm pore-size polycarbonate filters and resuspended in 0.6-1 mL Lauber buffer [50 mM HEPES (pH 7.3), 100 mM NaCl, 10 % sucrose, 0.1 % 3-(3-cholamidopropyl)-dimethylammonio-1-propanesulfonate, and 10 mM dithiothreitol] and sonicated on ice (four cycles of 30 seconds each) using an ultra-cell disruptor (Sonic Dismembrator, Fisher Scientific, Waltham, MA, USA). Cell extracts were centrifuged (10,000 x g, 2 min, room temperature) and supernatant was collected for caspase biochemical activity. Caspase-specific activity was determined by measuring the kinetics of cleavage for the canonical fluorogenic caspase substrate (Z-IETD-AFC) at a 50 mM final concentration (using Ex 400 nm and emission 505 nm; Synergy4 BioTek, Winooski, VT, USA), as previously described in Bar-Zeev et al. (2013). Fluorescence was converted to a normalized substrate

cleavage rate using an AFC standard (Sigma) and normalized to total protein concentrations obtained from the same samples. Total protein concentrations were determined by Pierce™ BCA Protein Assay Kit (Thermo Scientific product #23225).

2.9. 16S rRNA gene sequencing and data analyses

Bacterial community diversity was analyzed by deep sequencing of the 16S rRNA gene in samples from two replicate bottles from experiment 1 (see section 1.2) at three time points each. Seawater samples were filtered on 25 mm, 5 µm pore-size Supor filters (Pall Gelman Inc., Ann Arbor, Michigan), snap frozen in liquid nitrogen, and stored at -80 °C for later extraction. Community genomic DNA was isolated from the filters using a phenol–chloroform extraction method modified according to Massana et al. (1997). The 16S rRNA genes within community genomic DNA were initially amplified with conserved bacterial primers 27F and 1100R (Dowd et al., 2008) using a high fidelity polymerase (Phusion DNA polymerase, Thermo Scientific) with an initial denaturation step of 95 °C for 3 min followed by 20 cycles of 95 °C for 30 sec, 55 °C for 30 sec, and 72 °C for 45 sec. A secondary PCR (same conditions) was performed for next-generation sequencing by using customized fusion primers with different tag sequences. The tags were attached to the 27F primer and to the 338R primer (Hamady et al., 2008) to obtain 340 bp fragments suitable for IonTorrent analysis. The use of nested PCR was used to minimize inclusion of false sequences into the sequenced material (Dowd et al., 2008). After secondary PCR, all amplicon products were purified using Ampure magnetic purification beads (Agencourt Bio- science Corporation, MA, USA) to exclude primer-dimers. The amplicons were sequenced at the Bar-Ilan Sequencing Center, using an Ion Torrent™ (Life Technologies, USA).

The adapter-clipped sequences were processed using tools and scripts from the UPARSE pipeline (Edgar, 2013). Reads from all samples were pooled for OTU calling. Reads were demultiplexed, primers and barcodes stripped using the script *fastq_strip_barcode_relabel.py*, leaving 42747 raw reads altogether for six samples. As suggested for OTU calling from single-end amplicon sequences (Edgar, 2013), sequences (mostly between 280 nt and 300 nt) were trimmed to a fixed length of 280 nt, and shorter sequences were discarded (26740 trimmed raw reads remaining). For OTU clustering, trimmed raw reads were quality filtered using the *-fastq_filter* command with a maximum expected error rate (*-fastq_maxee*) of 2 (21590 reads remaining), clustered into unicals (100 % identity) and the unicals sorted by weight (number of sequences in the cluster). OTU clustering with an identity threshold of 0.98

was done using the *-cluster_otus* command on sorted unicals, with built-in chimera filtering. To infer OTU abundances for each individual sample, the trimmed raw reads per sample (after a more relaxed quality filtering with *-fastq_maxee* 5) were mapped back to these OTUs with *usearch_global* and a minimum identity of 98 %. For taxonomic classification, OTUs were submitted to <https://www.arb-silva.de/ngs/> and classified using the SINA aligner v1.2.10 and database release SSU 123 (Quast et al., 2013). Sequences having a $(BLAST\ alignment\ coverage + alignment\ identity)/2 < 93\%$ were considered as unclassified and assigned to the virtual group “No Relative” (5.58 % of OTUs).

2.10. RNA extraction and metatranscriptome sequencing

Metatranscriptomic sequencing was performed for three time points: peak surface accumulation of the bloom (T_0 , 12:00), 8 h (T_8 22:00), and 22 h (T_{22} 10:00) after T_0 . Cells on polycarbonate filters were resuspended in 1 mL PGTX [for 100 mL final volume: phenol (39.6 g), glycerol (6.9 mL), 8-hydroxyquinoline (0.1 g), EDTA (0.58 g), sodium acetate (0.8 g), guanidine thiocyanate (9.5 g), guanidine hydrochloride (4.6 g), Triton X-100 (2 mL)] (Pinto et al., 2009), and 250 µl glass beads (diameter 0.1 – 0.25 mm). and sonicated on a cell disruptor (Precellys, Peqlab, Germany) for 3 x 15 s at 6500 rpm. Tubes were placed on ice between each 15 s interval. RNA was extracted by adding 0.7 mL chloroform and subsequent phase separation. RNA was precipitated from the aqueous phase using 3 volumes of isopropanol at -20 °C overnight. Residual DNA was removed using the Turbo DNA-free Kit (Ambion) after the manufacturer’s instructions, but adding additional 1 µl of DNase after 30 min of incubation and incubating another 30 min. RNA was purified using Clean & Concentrator 5 columns (C&C 5) (Zymo Research, Freiburg, Germany). The pure RNA was treated with Ribo-Zero rRNA Removal Kit (Bacteria) (Epicentre, Madison, USA) and purified again with C&C 5. DNA contamination was tested and confirmed negative with a 40 cycle PCR using cyanobacteria-specific 16S primers.

For removal of tRNAs and small fragments, the RNA was purified with the Agencourt RNAClean XP kit (Beckman Coulter Genomics, Danvers, USA). First-strand cDNA synthesis for T_8 and T_{22} samples was primed with a N6 randomized primer, after which the cDNAs were fragmented by ultrasound (4 pulses of 30 sec at 4 °C). Illumina TruSeq sequencing adapters were ligated in a strand-specific way to the 5' and 3' ends and the resulting cDNAs were PCR-amplified to about 10-20 ng µL⁻¹ using a high fidelity DNA polymerase. Randomly-primed cDNA for T_0 samples was prepared using purified RNA without fragmentation followed by

ligation of Illumina TruSeq sequencing adapters to the 5' and 3' ends and fragmentation of cDNA > ~700 bp with ultrasound (4 pulses of 30 sec at 4°C; targeting only cDNA > 700 nt). After repairing ends, fragments were dA-tailed and Illumina TruSeq sequencing adapters were ligated again to the 5' and 3' ends of the cDNA and re-amplified. Consequently, a small fraction of the T₀ reads was not strand-specific. All cDNAs were purified using the Agencourt AMPure XP kit (Beckman Coulter Genomics, Danvers, USA) and 2 x 150 nt paired-end sequences generated with an Illumina NextSeq500 sequencer by a commercial provider (vertis AG, Freising, Germany).

2.11. Bioinformatics processing and analysis of metatranscriptome data

To remove adapters, perform quality trimming, and set a minimal length cutoff, raw fastq reads were processed with Cutadapt version 1.8.1 (Martin, 2011) in paired-end mode with a minimum adapter sequence overlap of 10 nt (-O 10), an allowed error rate of 20 % (-e 0.2) in the adapter sequence alignment, and a minimum base quality of 20. To remove residual ribosomal RNA reads, the fastq files were further processed with SortMeRNA version 1.8 (Kopylova et al., 2012) with the accompanying standard databases in paired end mode, resulting in 9,469,339 non-ribosomal reads for T₀, 22,407,194 for T₈, and 18,550,250 for T₂₂. The fastq files with all non-ribosomal forward-reads were used for mapping against the *Trichodesmium erythraeum* IMS101 genome with Bowtie2 (Langmead and Salzberg, 2012) in *very-sensitive-local* mode. This resulted in 51.9 % of T₀, 5.1 % of T₈, and 3.3 % of T₂₂ reads mapped. Reads were counted per CDS feature as annotated in the genome of *Trichodesmium erythraeum* (NC_008312.1) using htseq-count version 0.6.0 (Anders et al., 2014) and a count table generated with all read counts from T₀, T₈, and T₂₂.

For detection of differentially expressed genes from T₀ to T₈ and T₈ to T₂₂, the count table was processed with the statistical tool “Analysis of Sequence Counts” (ASC) (Wu et al., 2010). This tool is specifically designed to account for missing replicates by employing a model of biological variation of gene expression (Wu et al., 2010). The posterior probabilities (P) of a gene being > 2-fold differentially expressed (user specified threshold) between any two samples is calculated using an empirical Bayesian analysis algorithm and an internal normalization step. Differential expression of genes was defined as significant if P > 0.98.

3 Results

3.1. Setting the scene – *Trichodesmium* bloom development and bloom within the lagoon.

Trichodesmium were present as part of the *in-situ* community in the lagoon at the outset of the VAHINE experiment. (Bonnet et al., 2015; Turk-Kubo et al., 2015). In the lagoon water, temperatures were high ($> 25\text{ }^{\circ}\text{C}$) and typical oligotrophic conditions of austral summer prevailed. For the first 20 days of the experiment low abundance and biomass was measured for primary and secondary production and specifically for diazotrophic populations (Fig. 1). Total PON and POC in the lagoon fluctuated in the first 20 days of the VAHINE experiment with values ranging between $0.6\text{--}1.1\text{ }\mu\text{mol L}^{-1}$ and $5\text{--}11$ respectively. On the morning of day 23, values were 0.9 and $9.3\text{ }\mu\text{mol L}^{-1}$ PON and POC, respectively (Fig. 1c-d). The total Chl *a* concentrations ranged between $0.18\text{--}0.26\text{ }\mu\text{g L}^{-1}$ from days 1-20 (Fig. 1a). The increase in Chl *a* concentrations reflect the composite signature of the total phototrophic community [detailed in (Leblanc et al., 2016; Van Wambeke et al., 2015)] and is not specific to *Trichodesmium* biomass. Low abundances of *Trichodesmium* were measured in the lagoon waters throughout the first three weeks of the project (Turk-Kubo et al., 2015), with *Trichodesmium*-associated 16S counts ranging from 0.1 to $0.4\text{ }\%$ of the total number of 16S tags (Pfreundt et al., 2016). During the first eight days of sampling, *Trichodesmium* abundance as measured by *nifH* gene real-time PCR ranged from $3.4 \times 10^2\text{--}6.5 \times 10^3\text{ nifH copies L}^{-1}$. By days 14 and 16, *Trichodesmium* accounted for $15\text{ }\%$ of the total diazotroph population (with $1.1\text{--}1.5 \times 10^4\text{ nifH copies L}^{-1}$) increasing by day 22 to $42\text{ }\%$ of the diazotroph population ($1.4 \times 10^5\text{ nifH copies L}^{-1}$) (Turk-Kubo et al., 2015). By the morning of day 23, Chl *a* increased to $0.39\text{ }\mu\text{g L}^{-1}$ in the upper 1 m depth (Fig. 1a), yet *Trichodesmium* was still not visually observed at this time as a bloom on the sea surface. Phycoerythrin concentrations fluctuated between $0.1\text{--}0.4\text{ }\mu\text{g L}^{-1}$ during days 1-14 and then increased to a maximal peak of $> 0.8\text{ }\mu\text{g L}^{-1}$ on day 21 with values $\sim 0.5\text{ }\mu\text{g L}^{-1}$ on day 23 reflecting both the doubling in *Synechococcus* biomass (days 15-23) as well as increasing *Trichodesmium* (days 21-23) (Leblanc et al., 2016). N_2 fixation rates in the lagoon waters ranged between $0.09\text{--}1.2\text{ nmol N L}^{-1}\text{ h}^{-1}$ during the pre-bloom period (Fig. 1c) and on the morning of day 23 measured $0.5\text{ nmol L}^{-1}\text{ h}^{-1}$ (Fig. 1c). Zooplankton populations in the lagoon fluctuated around $5000\text{ individuals m}^{-3}$ and increased from day 9 to 16 to peak at $\sim 14000\text{ individuals m}^{-3}$ (Hunt et al., 2016). From day 16 to day 23 the total zooplankton population declined to $\sim 8000\text{ individuals m}^{-3}$ with harpacticoid copepods including grazers of *Trichodesmium* (*Macrosetella gracilis*, *Miracia efferata*, and *Oculosetella gracilis*) comprising $< 1.5\text{ }\%$ of total zooplankton community in the lagoon (Hunt et al., 2016). Virus like particles (VLP) ranged from $1\text{--}6 \times 10^6\text{ mL}^{-1}$ throughout the first

22 days of the VAHINE experiment and displayed a ~ 2-4 day oscillation (i.e., increasing for 2 days, then declining for the next 3 days, etc.) with mean values of $3.8 \times 10^6 \text{ mL}^{-1}$ (Fig. 1b). VLP counts in surface waters on day 23 were $1.8 \times 10^6 \text{ mL}^{-1}$ (Fig. 1b), just prior to the appearance of the *Trichodesmium* surface bloom. VLPs did not show any distinct correlations with total biomass indices such as PON and POC during the pre-bloom sampling (Fig. 1b-d). Depth-averaged dissolved inorganic phosphorus (DIP) concentrations in the lagoon waters were low at $0.039 \pm 0.001 \text{ } \mu\text{M}$, with a relatively stable DIP turnover time (T_{DIP}) of $1.8 \pm 0.7 \text{ d}$ for the first 15 days, that declined to 0.5 ± 0.7 by day 23 (Berthelot et al., 2015). Alkaline phosphatase activity (APA), which hydrolyzes inorganic phosphate from organic phosphorus, increased ~ 3 fold, from 1.8 ± 0.7 (average of days 1-4) to $5.0 \pm 1.4 \text{ nmole L}^{-1} \text{ h}^{-1}$ (average of days 19-23) (Van Wambeke et al., 2015) demonstrating a response in metabolic activity related to P acquisition for the microbial community probably related to the decreasing availability of DIP in the lagoon waters.

On day 23 (February 4) of the VAHINE measurements, dense surface accumulations of *Trichodesmium* were observed at midday (12:00 h) (Fig. 2a-c). Ambient air temperatures (~ 25 °C) increased to over 26 °C and the winds decreased to < 5 knots. These accumulations (hereafter blooms) appeared in the typical “slick” formations of dense biomass in ribbons visible on the surface seawater and spread out over tens of meters in the lagoon water outside the mesocosms (Fig. 2a-c). *Trichodesmium* abundance in these patches was extremely variable with Chl *a* concentrations exceeding 5 mg L^{-1} within dense patches and trichome abundance > 10,000 trichomes mL. These surface accumulations were visible and sampled again 5 h later (experiment 2), yet by the next morning, no such slicks or patches of dense biomass were observed or measured in the lagoon. The disappearance of the *Trichodesmium* in the lagoon water whether by drifting away, sinking to depth, or any other factor, prevented further investigation of these populations.

3.2. Investigating *Trichodesmium* mortality in experimental microcosms.

3.2.1 Changes in *Trichodesmium* biomass and associated microbial communities.

The spatially patchy nature of *Trichodesmium* blooms in the lagoon (Fig. 2a-c), and the rapid temporal modifications in water-column abundance of filaments and colonies probably induced (primarily) by physical drivers (turbulence and wind-stress), complicate *in-situ* sampling when targeting changes in specific biomass. To overcome this, we collected

Trichodesmium populations from the surface midday bloom and examined the physiological, biochemical, and genetic changes occurring with time until the biomass crashed ~ 24 h (see methods section 2.2) (Fig. 2 and Fig. 3). In these enclosed microcosms, *Trichodesmium* 16S copies comprised > 90 % of total copies (Fig. 3) enabling the use Chl *a* to follow changes in its biomass (Fig. 2f). Maximal Chl *a* concentrations in the incubations ($> 150 \pm 80 \mu\text{g L}^{-1}$; $n=6$) were measured at the start of the incubation soon after the biomass collection and resuspension in FSW. These *Trichodesmium* populations collapsed swiftly over the next day with Chl *a* concentrations declining to $24 \mu\text{g L}^{-1}$ and $11 \mu\text{g L}^{-1}$ Chl *a* after 10 and 22 h, respectively (Fig. 2f).

In experiment 1 we characterized the microbial community associated with the *Trichodesmium* biomass within the microcosms by 16S rRNA gene sequencing from two replicate bottles (experiment 1). At T_0 94 % and 93 % of the obtained 16S tags in both replicates (Fig. 3) were of the Oscillatoriales order (phylum Cyanobacteria), with 99.9 % of these sequences classified as *Trichodesmium* spp. (Fig. 3). In both replicates, the temporal decline of *Trichodesmium* biomass coincided with an increase in *Alteromonas* 16S tags, but this development temporally lagged in replicate 1 compared to replicate 2 (Fig. 3). Six hours (T_6) after the surface bloom was originally sampled (T_0), over 80 % of 16S tags from replicate 1 were characterized as *Trichodesmium*. 14 h after T_0 , Alteromonadales and Vibrionales replaced *Trichodesmium* now constituting only 9 % of 16S tags (Fig. 3). In replicate 2, *Trichodesmium* declined by 80 % 6 h after T_0 , with Alteromonadales and Flavobacteriales comprising the bulk of the biomass 18 hours after the start of incubations (Fig.3).

The rate of decline in *Trichodesmium* biomass within the 4.6 L microcosms paralleled that of *Trichodesmium* collected from the surface accumulations at 17:00 and incubated in 20 L carboys under ambient conditions for > 72 h (defined hereafter as experiment 2: Fig. 4). Here, *Trichodesmium* biomass decreased by > 80 % within 24 h of incubations with trichome abundance declining from $\sim 2500 \text{ trichomes mL}^{-1}$ at bloom collection to $\sim 495 \text{ trichomes mL}^{-1}$ (Fig. 4a). No direct correlation was observed between the decline of *Trichodesmium* and viral populations. VLP abundance at the time of the surface bloom sampling was at a maximum of $8.2 \times 10^6 \text{ mL}^{-1}$ (Fig. 4a), decreasing to $5.7 \times 10^6 \text{ mL}^{-1}$ in the next 4 h then remaining stable throughout the crash period (within the next 42 h) averaging $\sim 5 \times 10^6 \pm 0.7 \text{ mL}^{-1}$ (Fig. 4a).

As *Trichodesmium* crashed in the experimental incubations, high values of NH_4^+ were measured (Fig 4b). In experiment 2, NH_4^+ increased exponentially from $73 \pm 0.0004 \text{ nmol}$

$\text{NH}_4^+ \text{ L}^{-1}$ when the surface bloom was collected and placed in the carboys (17:00 h) to 1490 ± 686 after 24 h and values $> 5000 \text{ nmol L}^{-1}$ 42 h after the incubation start (Fig. 3b). The high ammonia declined somewhat by the end of the experiment (after 72 h), yet was still high at $3494 \pm 834 \text{ nmol L}^{-1}$. Concurrently with the high NH_4^+ concentrations, and despite the dying *Trichodesmium*, we measured an increase N_2 -fixation rates. N_2 -fixation rose from $1.5 \text{ nmol N L}^{-1} \text{ h}^{-1}$ at T_0 to $3.5 \pm 2.8 \text{ nmol N L}^{-1} \text{ h}^{-1}$ 8 h after incubations began and $11.7 \pm 3.4 \text{ nmol N L}^{-1}$ 24 h later (Fig 4b). These high values represent other diazotrophs including UCYN-types and diatom-diazotroph associations that flourished after the *Trichodesmium* biomass had declined in the carboys (Bonnet et al. 2016b; Turk-Kubo personal communication). POC and PON, representing the fraction of C and N incorporated into biomass, ranged between $5.2\text{-}11.2 \text{ }\mu\text{mol C L}^{-1}$ and $0.6\text{-}1.1 \text{ }\mu\text{mol N L}^{-1}$ during pre-bloom periods (Fig. 1b) and $12.6 \pm 4.6 \text{ }\mu\text{mol C L}^{-1}$ and $1.3 \pm 0.5 \text{ }\mu\text{mol N L}^{-1}$ when the surface bloom was sampled (Fig. 4b-c). 24 hours after collection of bloom biomass POC increased ~ 6 -fold to $63.2 \pm 15 \text{ }\mu\text{mol C L}^{-1}$ and PON increased 10-fold to $10 \pm 3.3 \text{ }\mu\text{mol N L}^{-1}$ (Fig. 4b-c). After 72 h, total POC was $62 \pm 4 \text{ }\mu\text{mol C L}^{-1}$ (Fig. 4c) and PON increased to $14.1 \pm 6 \text{ }\mu\text{mol N L}^{-1}$ (Fig. 4b).

Organic carbon in the form of TEP is secreted when *Trichodesmium* is stressed and undergoing PCD (Bar-Zeev et al., 2013; Berman-Frank et al., 2004). TEP concentrations in the lagoon waters during the pre-bloom period (first 20 days) fluctuated around $\sim 350 \text{ }\mu\text{g gum xanthan (GX) L}^{-1}$ (Fig. 1d) that increased to $\sim 500 \text{ }\mu\text{g GX L}^{-1}$ on day 22 (Fig. 1d). During the time of biomass collection from the surface bloom TEP concentration exceeded $700 \text{ }\mu\text{g GX L}^{-1}$ (Fig. 4c). After biomass enclosure (experiment 2) TEP concentrations declined to $420 \pm 35 \text{ }\mu\text{g GX L}^{-1}$ and subsequently to $180 \pm 25 \text{ }\mu\text{g GX L}^{-1}$ 42 h and 72 h after T_0 (Fig. 4c).

3.2.2. Genetic responses of stressed *Trichodesmium*

Metatranscriptomic analyses of the *Trichodesmium* biomass were conducted in samples from experiment 1, at T_0 , T_8 , and T_{22} (Fig. S1). We examined differential expression during this period by investigating a manually curated gene suite including specific pathways involved in P and Fe uptake and assimilation, PCD, or gas vesicle synthesis. Genes involved in the acquisition and transport of inorganic and organic P sources were upregulated, concomitant with biomass demise; significantly higher expression levels were evident at T_8 and T_{22} compared to T_0 (Table S1). Abundance of alkaline phosphatase transcripts, encoded by the *phoA* gene (Orchard et al., 2003), increased significantly (~ 5 fold) from T_0 to T_{22} (Fig. 5a). The transcript abundance of phosphonate transporters and C-P lyase genes (*phnC*, *phnD*,

phnE, *phnH*, *phnI*, *phnL* and *phnM*) increased significantly (5-12 fold) between T₀ and both T₈ and T₂₂ (Fig. 5a, Table S1). Of the phosphite uptake genes, only *ptxA* involved in the phosphite (reduced inorganic phosphorus compound) uptake system, and recently found to operate in *Trichodesmium* (Martínez et al., 2012; Polyviou et al., 2015) was significantly upregulated at both T₈ and T₂₂ compared to T₀ (4.5 and 7 fold change respectively). The two additional genes involved in phosphite uptake, *ptxB* and *ptxC*, did not change significantly, as *Trichodesmium* biomass crashed (Fig. 5a).

Fe limitation induces PCD in *Trichodesmium* (Berman-Frank et al., 2004; Berman-Frank et al., 2007) we therefore examined genetic markers of Fe stress. At the time of surface bloom sampling (experiment 1, T₀), Fe stress was indicated by higher differential expression of several genes. The *isiB* gene encodes flavodoxin and serves as a common diagnostic indicator of Fe stress in *Trichodesmium*, since it may substitute for Fe-S containing ferredoxin (Bar-Zeev et al., 2013; Chappell and Webb, 2010). Transcripts of *isiB* were significantly higher at T₀ (3-fold) than at T₈ and T₂₂ (Fig. 5b, Table S1). The chlorophyll-binding protein IsiA is induced in cyanobacterial species under Fe or oxidative stress to prevent oxidative damage (Laudenbach and Straus, 1988). Here *isiA* transcripts increased 2- and 3- fold from T₀ to T₈ and T₂₂, respectively (Fig. 5b, Table S1). The Fe transporter gene *idiA* showed a transient higher transcript accumulation only at T₈. As the health of *Trichodesmium* declined, transcripts of the Fe-storage protein ferritin (*Dps*) decreased by > 70 % at T₂₂ (Fig. 5b, Table S1)

3.2.3. PCD-induced demise.

Our earlier work demonstrating PCD in *Trichodesmium* allowed us to utilize two independent biomarkers to investigate PCD induction during *Trichodesmium* demise, namely changes in catalytic rates of caspase-specific activity (Berman-Frank et al., 2004; Berman-Frank et al., 2007) and levels of metacaspase transcript expression (Bar-Zeev et al., 2013). When the surface bloom was sampled (experiment 1, T₀), protein normalized caspase-specific activity was 0.23 ± 0.2 pmol mg protein⁻¹ min⁻¹ (Fig. 6a). After a slight decline in the first 2 h, caspase activity increased throughout the experiment with 10 fold higher values (2.9 ± 1.5 pmol L⁻¹ mg protein⁻¹ min⁻¹) obtained over the next 22 h as the bloom crashed (Fig. 6a).

We followed transcript abundance over the demise period for the 12 identified metacaspase genes in *Trichodesmium* [(Asplund-Samuelsson et al., 2012; Asplund-Samuelsson, 2015; Berman-Frank et al., 2004)]; *TeMC1* (Tery_2077), *TeMC2* (Tery_2689), *TeMC3* (Tery_3869),

TeMC4 (Tery_2471), *TeMC5* (Tery_2760), *TeMC6* (Tery_2058), *TeMC7* (Tery_1841), *TeMC8* (Tery_0382), *TeMC9* (Tery_4625), *TeMC10* (Tery_2624), *TeMC11* (Tery_2158), and *TeMC12* (Tery_2963)] (Fig. 6b, Table S1). A subset of these genes was previously implicated in PCD of *Trichodesmium* cultures in response to Fe and light stress (Bar-Zeev et al., 2013; Berman-Frank et al., 2004; Bidle, 2015). Here, we interrogated the entire suite of metacaspases in natural *Trichodesmium* populations. As the biomass crashed from T₀ to T₂₂, 7 out of 12 metacaspases (*TeMC1*, *TeMC3*, *TeMC4*, *TeMC7*, *TeMC8*, *TeMC9*, and *TeMC11*) were significantly upregulated 8 and 22 h after T₀ (Fig. 6b). For these genes, transcript abundance increased 2.3- to 5.3-fold 8 h after T₀ and 3.5-6.2-fold 22 h after T₀ (Fig. 6b, Table S1) *TeMC5* and *TeMC10* transcripts increased significantly after 22 h by 2.9- and 3.2 fold, respectively. *TeMC6* was upregulated 2.9-fold after 8 h. *TeMC2* transcripts did not significantly change over time. We did not detect any expression of *TeMC12* throughout the experiment.

Export flux can be enhanced by PCD-induced sinking (Bar-Zeev et al., 2013) as PCD in *Trichodesmium* results in degradation of internal components, especially gas vesicles that are required for buoyancy (Berman-Frank et al., 2004). Although we did not measure changes in buoyancy itself, we observed rapid sinking of the *Trichodesmium* biomass in the bottles and carboys. The metatranscriptomic analyses demonstrated that, excluding one copy of *gvpL/gvpF*, encoding a gas vesicle synthesis protein, gas vesicle protein (*gvp*) genes involved in gas-vesicle formation (*gvpA*, *gvpN*, *gcpK*, *gvpG* and *gvpL/gcpF*) were all significantly downregulated relative to T₀ (Fig. 7, Table S1).

4 Discussion

4.1. Mortality processes of *Trichodesmium* – incubation results.

4.1.1 Grazer and virus influence.

Our microcosm incubations allowed us to specifically focus on the loss factors and show the involvement of biotic and abiotic stressors in inducing PCD and mechanistically impacting the demise and fate of a natural *Trichodesmium* bloom. We appreciate that the enclosure of the biomass in bottles and carboys may accelerate the processes occurring in the natural lagoon setting. Yet, the published rates of *Trichodesmium* mortality from field studies (Rodier and Le Borgne, 2010) indicate that these can parallel our loss rates with natural bloom demise occurring 24-48 h after peak of biomass.

We focused initially on biotic factors that could impact the incubated *Trichodesmium* biomass. The low number of harpacticoid zooplankton specific to *Trichodesmium* (O'Neil and Roman, 1994; O'Neil, 1998) in the lagoon (Hunt et al., 2016) and especially those in the bottles (personal observation) refutes the hypothesis that grazing caused the massive mortality of *Trichodesmium* biomass in our experimental incubations.

Viruses have been increasingly invoked as key agents terminating phytoplankton blooms (Brussaard et al., 2005; Jacquet et al., 2002; Lehahn et al., 2014; Tarutani et al., 2000; Vardi et al., 2012). In *Trichodesmium*, phages have been implicated in bloom crashes, but this mechanism has yet to be unequivocally proven (Hewson et al., 2004; Ohki, 1999); indeed, no specific *Trichodesmium* phage has been isolated or characterized to date (Brown et al., 2013). Here, total VLP abundance was highest at the time of sampling from the surface *Trichodesmium* bloom and at the start of the incubation at $\sim 8 \times 10^6$ VLPs mL⁻¹ it actually declined 2 fold in the first eight hours of incubation before increasing over the next 32 h (Fig. 4a). While our method of analysis cannot distinguish between phages infecting *Trichodesmium* from those infecting other marine bacteria, it argues against a massive, phage-induced lytic event of *Trichodesmium*. Such an event would have yielded a notable burst of VLPs upon bloom crash, especially considering the high *Trichodesmium* biomass observed. The coincidence between the maximal abundance of VLPs and highest *Trichodesmium* biomass is counter to viruses serving as the mechanism of mortality in our incubation experiments. Nonetheless, virus infection itself may be a stimulant for community N₂ fixation perhaps by releasing key nutrients (i.e., P or Fe) upon lysis of surrounding microbes (Weitz and Wilhelm, 2012). Although we did not characterize them here, it is indeed possible that *Trichodesmium*-specific phages were present in our incubation experiments and they may have exerted additional physiological stress on resident populations, facilitating PCD induction. Virus infection increases the cellular production of reactive oxygen species (ROS) (Evans et al., 2006; Vardi et al., 2012), which in turn can stimulate PCD in algal cells (Berman-Frank et al., 2004; Bidle, 2015; Thametrakoln et al., 2012). Viral attack can also directly trigger PCD as part of an antiviral defense system activated to limit virus production and prevent massive viral infection (Bidle and Falkowski, 2004; Bidle, 2015; Georgiou et al., 1998).

4.1.2 Stressors impacting mortality.

Nutrient stress can be acute or chronic to which organisms may acclimate on different time scales. Thus, for example, the consistently low DIP concentrations measured in the lagoon

during the 22 days preceding the *Trichodesmium* surface bloom probably enabled acclimation responses such as induction of APA and other P acquisition systems. *Trichodesmium* has the ability to obtain P via inorganic and organic sources including methylphosphonate, ethylphosphonate, 2-aminoethylphosphonate (Beversdorf et al., 2010; Dyhrman et al., 2006), and via a phosphite uptake system (PtxABC) that accesses P via the reduced inorganic compound phosphite (Martínez et al., 2012; Polyviou et al., 2015). Our metatranscriptomic data demonstrated upregulated expression of genes related to all three of these uptake systems (DIP, phosphonates, phosphites) 8 and 22 h after incubation began, accompanying biomass demise (Fig. 5a). This included one gene for phosphite uptake (*ptxA*) and several genes from the phosphonate uptake operon (*phnDCEEGHIJKLM*) (Hove-Jensen et al., 2014). Upregulated expression of *phnD*, *phnC*, *phnE*, *phnH*, *phnI*, *phnJ*, *phnK*, *phnL* and *phnM* occurred as the *Trichodesmium* biomass crashed (Fig. 5a, Table S1), consistent with previous results demonstrating that *phnD* and *phnJ* expression levels increased during DIP depletion (Hove-Jensen et al., 2014). It is likely that during bloom demise, the C-P lyase pathway of remaining living cells was induced when DIP sources were extremely low, while POP and DOP increased along with the decaying organic matter. The ability to use phosphonates or phosphites as a P source can provide a competitive advantage for phytoplankton and bacteria in P-depleted waters (Coleman and Chisholm, 2010; Martinez et al., 2010). Thus, it is puzzling why dying cells would upregulate *phn* genes or *phoA* transcripts after 22 h incubation (Fig. 5a). A more detailed temporal resolution of the metatranscriptomic analyses may elucidate the expression dynamics of these genes and their regulating factors. Alternatively, in PCD-induced populations, a small percentage remains viable and resistant as either cysts (Vardi et al., 1999) or hormogonia (Berman-Frank et al., 2004) that can serve as the inoculum for future blooms. It is plausible that the observed upregulation signal was attributable to these sub-populations.

The concentrations of dissolved and bioavailable Fe were not measured in the lagoon water during the experimental period as Fe is typically replete in the lagoon (Jacquet et al., 2006). However, even in Fe-replete environments such as the New Caledonian lagoon, dense patches of cyanobacterial or algal biomass can deplete available resources and cause limited micro-environments (Shaked, 2002). We obtained evidence for Fe stress using several proxy genes demonstrating that enhanced cellular Fe demand occurred during the bloom crash (Table S1). *Trichodesmium*'s strategies of obtaining and maintaining sufficient Fe involves genes such as *isiB*. *isiB* was highly expressed when biomass accumulated on the surface waters, indicative

for higher Fe demand at this biomass load (Bar-Zeev et al., 2013; Chappell and Webb, 2010). Transcripts for chlorophyll-binding, Fe-stress-induced protein A (*IsiA*) increased (albeit not significantly) 3-fold over 22 h of bloom demise (Fig. 5b, Table S1). In many cyanobacteria, *isiA* expression is stimulated under Fe stress (Laudenbach and Straus, 1988) and oxidative stress (Jeanjean et al., 2003) and functions to prevent high-light induced oxidative damage by increasing cyclic electron flow around the photosynthetic reaction center photosystem I (Havaux et al., 2005; Latifi et al., 2005; Michel and Pistorius, 2004). Dense surface blooms of *Trichodesmium* are exposed to high irradiance (on day 23 average PAR was 3000 $\mu\text{mol photons m}^{-2} \text{s}^{-1}$). It is possible that high Fe demand combined with the oxidative stress of the high irradiance induced the higher expression of *isiA* (Fig. 5b). As cell density and associated self-shading of *Trichodesmium* filaments decreased during bloom crash, light-induced oxidative stress is likely the principal driver for elevated *isiA* expression.

The gene *idiA* is another environmental Fe stress biomarker that allows acquisition and transfer of Fe through the periplasm into the cytoplasm (Chappell and Webb, 2010). In our incubation, upregulated expression of *idiA* (an ABC Fe⁺³ transporter) was evident after 8 h. This is consistent with increasing Fe-limitation, as *Trichodesmium* abundance (measured via 16S rRNA gene sequencing) was still high at T₆ (after 6 h of incubations) (replicate 1). These findings are consistent with proteomics analyses from deplete iron (0 μM Fe) *Trichodesmium* cultures which revealed an increase in IdiA protein expression (Snow et al., 2015). Lastly, our metatranscriptomic data highlighted a reduction in Fe storage and utilization, as the expression of Fe-rich ferritin-like DPS proteins (Castruita et al., 2006), encoded by *dpsA*, decreased ~ 5 fold by the time that most of the biomass had crashed (T₂₂) (Fig. 5b, Table S1). *dpsA* was also downregulated under Fe-replete conditions in *Synechococcus* (Mackey et al., 2015), but the downregulation observed here is more likely related to *Trichodesmium* cells dying and downregulating Fe-demanding processes such as photosynthesis and N₂ fixation.

4.1.3. Programmed cell death (PCD) and markers for increased export flux.

The physiological and morphological evidence of PCD in *Trichodesmium* has been previously documented in both laboratory (Bar-Zeev et al., 2013; Berman-Frank et al., 2004) and environmental cultures collected from surface waters around New Caledonia (Berman-Frank et al., 2004). Here, we confirmed characteristic features of autocatalytic PCD in *Trichodesmium* such as increased caspase-specific activity (Fig. 6a), globally enhanced metacaspase expression (Fig. 6b), and decreased expression of gas vesicle maintenance (Fig.

7). Metatranscriptomic snapshots interrogating expression changes in all *Trichodesmium* metacaspases (Fig. 6b) generally portrayed upregulated expression concomitant with biomass decline. Our results are consistent with previous observations that Fe-depleted PCD-induced laboratory cultures of *Trichodesmium* IMS101 had higher expression levels of *TeMCI* and *TeMC9* compared to healthy Fe-replete cultures (Bar-Zeev et al., 2013; Berman-Frank et al., 2004). To our knowledge, this is the first study examining expression levels of metacaspases in environmental *Trichodesmium* samples during a natural bloom. 11 of the 12 annotated metacaspases in *Trichodesmium* were expressed in all 3 metatranscriptomes from the surface bloom. To date, no specific function has been determined for these metacaspases in *Trichodesmium* other than their association with cellular stress and death. Efforts are underway to elucidate the specific cellular functions, regulation, and protein interactions of these *Trichodesmium* metacaspases (Pfreundt et al., 2014; Spungin et al., In prep).

In cultures and isolated natural populations of *Trichodesmium*, high caspase-like specific activity is correlated with the initial induction stages of PCD with activity declining as the biomass crashes (Bar-Zeev et al., 2013; Berman-Frank et al., 2004; Berman-Frank et al., 2007). Here, caspase-like activity increased with the crashing populations of *Trichodesmium* (Fig. 5a). Notably, maximal caspase activities were recorded at T₂₃, after which most *Trichodesmium* biomass had collapsed. The high protein-normalized caspase-specific activity may be a result of a very stressed and dying sub-population of *Trichodesmium* that had not yet succumbed to PCD (Berman-Frank et al., 2004). Alternatively, the high caspase-like activity may be attributed to the large population of *Alteromonas* bacteria that were associated with the remaining detrital *Trichodesmium* biomass. However, currently, we are unaware of any publications demonstrating high cellular caspase-specific activity in clades of γ -Proteobacteria.

Gas vesicles are internal structures essential for maintaining buoyancy of *Trichodesmium* populations in the upper surface waters enabling them to vertically migrate and respond to light and nutrient requirements (Capone et al., 1997; Walsby, 1978). Mortality via PCD causes a decline in the number and size of cellular gas vesicles in *Trichodesmium* (Berman-Frank et al., 2004) and results in an enhanced vertical flux of trichomes and colonies to depth (Bar-Zeev et al., 2013). Our metatranscriptomic data supported the subcellular divestment from gas vesicle production during bloom decline, as the expression of vesicle-related genes was downregulated (Fig. 7). In parallel, TEP production and concentration increased to > 800 $\mu\text{g GX L}^{-1}$, a 2-fold increase from pre-bloom periods (Fig. 1d and Fig. 4c). When nutrient uptake

is limited, but CO₂ and light are sufficient, uncoupling occurs between photosynthesis and growth (Berman-Frank and Dubinsky, 1999), leading to increased production of excess polysaccharides, such as TEP, and corresponding with high TEP found in bloom decline phases rather than during the increase in population density (Engel, 2000; Smetacek, 1985). In earlier studies we demonstrated that PCD-induced demise in *Trichodesmium* is characterized by an increase in excreted TEP, (Berman-Frank et al., 2007) and enhanced sinking of particulate organic matter (Bar-Zeev et al., 2013). TEP itself may be positively buoyant (Azetsu-Scott and Passow, 2004), yet its stickiness causes aggregation and clumping of cells and detritus, ultimately enhancing sinking rates of large aggregates including dying *Trichodesmium* (Bar-Zeev et al., 2013).

4.1.4. Changes in microbial community with *Trichodesmium* decline.

In the incubations, other diazotrophic populations succeeded the declining *Trichodesmium* biomass as indicated by increasing N₂ fixation rates, POC, and PON (Fig. 4b). In experiment 2, based on qPCR of targeted diazotrophic phylotypes, the diazotroph community composition shifted from being dominated by *Trichodesmium* spp. and unicellular groups UCYN-A1, UCYN-A2, and UCYN-B (T₀), to one dominated by diatom-diazotroph associations Het-1 and Het-2 (T₇₂) (Bonnet et al. 2016b; Turk-Kubo, personal communication). In experiment 1 heterotrophic bacteria thrived and increased in abundance as the *Trichodesmium* biomass crashed (Fig. 3).

Trichodesmium colonies host a wide diversity of microorganisms including specific epibionts, viruses, bacteria, eukaryotic microorganisms and metazoans (Hewson et al., 2009; Hmelo et al., 2012; Ohki, 1999; Paerl et al., 1989; Sheridan et al., 2002; Siddiqui et al., 1992; Zehr, 1995). Associated epibiont bacterial abundance in dilute and exponentially growing laboratory cultures of *Trichodesmium* is relatively limited (Spungin et al., 2014) compared to bloom conditions (Hewson et al., 2009; Hmelo et al., 2012). Proliferation of *Alteromonas* and other γ -Proteobacteria during biomass collapse (Fig. 3) confirms their reputation as opportunistic microorganisms (Allers et al., 2008; Hewson et al., 2009; Frydenborg et al., 2014; Pichon et al., 2013). Such organisms can thrive on the influx of organic nutrient sources from the decaying *Trichodesmium* as we observed (Fig. 3). Furthermore, the increase of organic matter including TEP produced by the stressed *Trichodesmium* (Fig. 1d and Fig. 4c) probably stimulated growth of these copiotrophs. Moreover, as the *Trichodesmium* biomass declined in the carboys, the high concentrations of NH₄⁺ (> 5000 nmol L⁻¹) (Fig. 4b) sustained both autotrophic and heterotrophic organisms (Berthelot et al., 2015; Bonnet et al., 2015; Bonnet

et., 2016b). Thus, the increase in volumetric N₂ fixation and PON that was measured in the incubation bottles right after the *Trichodesmium* crash in experiment 2 (Fig 4b) probably reflects both the enhanced activity of other diazotrophs (see above and Bonnet et al. 2016b) and resistant residual *Trichodesmium* trichomes (Berman-Frank et al. 2004) with increased cell specific N₂ fixation. This scenario is consistent with the hypothesis that PCD induction and death of a fraction of the population confers favorable conditions for survival and growth of individual cells (Bidle and Falkowski, 2004).

4.2. Implications for the lagoon system and export flux.

Phytoplankton blooms and their dense surface accumulations occur under favorable physical properties of the upper ocean (e.g. temperature, mixed-layer depth, stratification) and specifically when division rates exceed loss rates derived from grazing, viral attack, and sinking or export from the mixed layer to depth (Behrenfeld, 2014). Although physical drivers such as turbulence and mixing may scatter and dilute these dense accumulations, the rapid disappearance of biomass in large sea-surface *Trichodesmium* blooms (within 1-2 d in the lagoon waters) (Rodier and Le Bourne 2010) suggests loss of biomass by other mechanisms. The lack of *Trichodesmium* developing within the VAHINE mesocosms and the spatial-temporal variability of the surface bloom in the lagoon prohibited *in-situ* sampling of the same biomass for several days and prevented conclusions regarding *in-situ* mortality rates and export flux. Furthermore, within these dense surface populations as well as in the microcosm and carboy experiments, nutrient availability was probably extremely limited due to high demand and competition (Shaked 2002). PCD induced by Fe-depletion experiments with laboratory cultures and natural populations results in rapid biomass demise typically beginning after 24 h with > 90 % of the biomass crashing 3 to 5 days after induction (Bar-Zeev et al., 2013; Berman-Frank et al., 2004; Berman-Frank et al., 2007). In similar experiments with P-depletion, *Trichodesmium* biomass did not crash rapidly. Rather, limitation induced colony formation and elongation of trichomes (Spungin et al., 2014) and the cultures could be sustained for another couple of weeks before biomass declined significantly (unpublished data). The responses we quantified from the dying *Trichodesmium* in the carboys and bottles (Fig. 3-7) were similar to those obtained from controlled laboratory experiments where the nutrient stressors P and Fe were validated individually. However, the rapid response here probably reflects an exacerbated reaction due to the simultaneous combination of different stressors and the presence of biotic components that can compete for and utilize the organic resources (carbon, nitrogen, phosphorus) generated by the dying *Trichodesmium*. In the

lagoon, production of TEP by stressed biomass combined with the degradation of gas vesicles and enhanced aggregation will cause such surface accumulations or blooms to collapse leading to rapid vertical export of newly fixed nitrogen and carbon in the ocean.

5 Conclusions and implications

We demonstrate that the rapid demise of a *Trichodesmium* surface bloom in New Caledonia, with the disappearance of > 90 % of the biomass within 24 h in 4.5 L bottle incubations, displayed cellular responses to P and Fe stress and was mediated by a suite of PCD genes. Virus infection and lysis did not appear to directly cause the massive biomass decline. Although virus infection may have modulated the cellular and genetic responses to enhance PCD-driven loss processes. Quorum sensing among epibionts (Hmelo et al., 2012; Van Mooy et al., 2012), allelopathic interactions, and the production of toxins by *Trichodesmium* (Guo and Tester, 1994; Kerbrat et al., 2010) are additional factors that could be important for a concerted response of the *Trichodesmium* population, yet we did not examine them here. Collectively, they would facilitate rapid collapse and loss of *Trichodesmium* populations, and possibly lead to enhanced vertical fluxes and export production, as previously demonstrated in PCD-induced laboratory cultures of *Trichodesmium* (Bar-Zeev et al., 2013). We posit that PCD induced demise, in response to concurrent cellular stressors, and facilitated by concerted gene regulation, is typical in natural *Trichodesmium* blooms and leads to a high export production rather than regeneration and recycling of biomass in the upper photic layers.

Author contributions

IBF, DS, and SB conceived and planned the study. DS, UP, HB, SB, WRH, KB and IBF participated in the experimental sampling. DS, UP, WRH, HB, FN, DAR, KB, and IBF analyzed the samples and resulting data. IBF and DS wrote the manuscript with further contributions to the manuscript by UP, WRH, SB, and KB.

Acknowledgments

Funding was obtained for IBF through a collaborative grant from MOST Israel and the High Council for Science and Technology (HCST)-France, and a United States-Israel Binational Science Foundation (BSF) grant (No: 2008048) to IBF and KB. This research was partially

funded by the Gordon and Betty Moore Foundation through Grant GBMF3789 to KDB. The participation of IBF, DS, UP, and WRH in the VAHINE experiment was supported by the German-Israeli Research Foundation (GIF), project number 1133-13.8/2011 to IBF and WRH, and the metatranscriptome analysis by the EU project MaCuMBA (Marine Microorganisms: Cultivation Methods for Improving their Biotechnological Applications; grant agreement no: 311975) to WRH. Funding for VAHINE Experimental project was provided by the Agence Nationale de la Recherche (ANR starting grant VAHINE ANR-13-JS06-0002), INSU-LEFE-CYBER program, GOPS, IRD and M.I.O. The authors thank the captain and crew of the R/V Alis, SEOH divers service from the IRD research center of Noumea (E. Folcher, B. Bourgeois and A. Renaud) and from the Observatoire Océanologique de Villefranche-sur-mer (OOV, J.M. Grisoni), and technical service of the IRD research center of Noumea for their helpful technical support. Thanks especially to E. Rahav for his assistance throughout the New Caledonia experiment and to H. Elifantz for assistance with the 16S sequencing and data analysis. This work is in partial fulfillment of the requirements for a PhD thesis for D. Spungin at Bar-Ilan University. We thank the three reviewers whose comments helped improve the manuscript substantially.

References

- Allers, E., Niesner, C., Wild, C., and Pernthaler, J.: Microbes enriched in seawater after addition of coral mucus, *Applied and Environmental Microbiology*, 74, 3274-3278, 2008.
- Anders, S., Pyl, P. T., and Huber, W.: HTSeq—A Python framework to work with high-throughput sequencing data, *Bioinformatics*, btu638, 2014.
- Asplund-Samuelsson, J., Bergman, B., and Larsson, J.: Prokaryotic caspase homologs: phylogenetic patterns and functional characteristics reveal considerable diversity, *PLOS One*, 7, e49888, 2012.
- Asplund-Samuelsson, J.: The art of destruction: revealing the proteolytic capacity of bacterial caspase homologs, *Molecular Microbiology*, 98, 1-6, 2015.
- Azetsu-Scott, K., and Passow, U.: Ascending marine particles: Significance of transparent exopolymer particles (TEP) in the upper ocean, *Limnology and Oceanography*, 49, 741-748, 2004.

766 Bar-Zeev, E., Avishay, I., Bidle, K. D., and Berman-Frank, I.: Programmed cell death in the
767 marine cyanobacterium *Trichodesmium* mediates carbon and nitrogen export, The ISME
768 Journal, 7, 2340-2348, 2013.

769 Behrenfeld, M. J.: Climate-mediated dance of the plankton, Nature Climate Change, 4, 880-
770 887, 2014.

771 Bergman, B., Sandh, G., Lin, S., Larsson, J., and Carpenter, E. J.: *Trichodesmium* - a
772 widespread marine cyanobacterium with unusual nitrogen fixation properties, FEMS
773 Microbiology Reviews, 1-17, 10.1111/j.1574-6976.2012.00352.x., 2012.

774 Berman-Frank, I., and Dubinsky, Z.: Balanced growth in aquatic plants: Myth or reality?
775 Phytoplankton use the imbalance between carbon assimilation and biomass production to their
776 strategic advantage, Bioscience, 49, 29-37, 1999.

777 Berman-Frank, I., Cullen, J. T., Shaked, Y., Sherrell, R. M., and Falkowski, P. G.: Iron
778 availability, cellular iron quotas, and nitrogen fixation in *Trichodesmium*, Limnology and
779 Oceanography, 46, 1249-1260, 2001.

780 Berman-Frank, I., Bidle, K., Haramaty, L., and Falkowski, P. G.: The demise of the marine
781 cyanobacterium, *Trichodesmium* spp., via an autocatalyzed cell death pathway, Limnology
782 and Oceanography, 49, 997-1005, 2004.

783 Berman-Frank, I., Rosenberg, G., Levitan, O., Haramaty, L., and Mari, X.: Coupling between
784 autocatalytic cell death and transparent exopolymeric particle production in the marine
785 cyanobacterium *Trichodesmium*, Environmental Microbiology, 9, 1415-1422, 10.1111/j.1462-
786 2920.2007.01257.x, 2007.

787 Berthelot, H., Moutin, T., L'Helguen, S., Leblanc, K., Hélias, S., Grosso, O., Leblond, N.,
788 Charrière, B., and Bonnet, S.: Dinitrogen fixation and dissolved organic nitrogen fueled
789 primary production and particulate export during the VAHINE mesocosm experiment (New
790 Caledonia lagoon), Biogeosciences, 12, 4099-4112, 10.5194/bg-12-4099-2015, 2015.

791 Beversdorf, L., White, A., Björkman, K., Letelier, R., and Karl, D.: Phosphonate metabolism
792 by *Trichodesmium* IMS101 and the production of greenhouse gases, Limnology and
793 Oceanography, 55, 1768-1778, 2010.

794 Bidle, K. D., and Falkowski, P. G.: Cell death in planktonic, photosynthetic microorganisms,
795 Nature Reviews Microbiology, 2, 643-655, 2004.

796 Bidle, K. D.: The molecular ecophysiology of programmed cell death in marine
797 phytoplankton, Annual Review Marine Science, 7, 341-375, 2015.

798 Bonnet, S., Berthelot, H., Turk-Kubo, K., Fawcett, S., Rahav, E., l'Helguen, S., and Berman-
799 Frank, I.: Dynamics of N₂ fixation and fate of diazotroph-derived nitrogen in a low nutrient
800 low chlorophyll ecosystem: results from the VAHINE mesocosm experiment (New
801 Caledonia), Biogeosciences, 12, 19579-19626, doi:10.5194/bgd-12-19579-2015, 2015.

802 Bonnet, S., Moutin, T., Rodier, M., Grisoni, J. M., Louis, F., Folcher, E., Bourgeois, B., Boré,
803 J. M., and Renaud, A.: Introduction to the project VAHINE: Variability of vertical and trophic
804 transfer of diazotroph derived N in the South West Pacific, Biogeosciences, doi:10.5194/bg-
805 2015-615, 2016a.

806 Bonnet, S., Berthelot, H., Turk-Kubo, K., Cornet-Barthaux, V., Fawcett, S., Berman-Frank, I.,
 807 Barani, A., Dekeazemacker, J., Benavides, M., Charrière, B., and Capone, D.: *Trichodesmium*
 808 blooms support diatom growth in the Southwest Pacific Ocean, Limnology and
 809 Oceanography, 2016b. In Press.
 810
 811 Brown, J. M., LaBarre, B. A., and Hewson, I.: Characterization of *Trichodesmium*-associated
 812 viral communities in the eastern Gulf of Mexico, FEMS Microbiology Ecology, 84, 603-613,
 813 2013.
 814
 815 Brussaard, C. P. D., Mari, X., Van Bleijswijk, J. D. L., and Veldhuis, M. J. W.: A mesocosm
 816 study of *Phaeocystis globosa* (Prymnesiophyceae) population dynamics - II. Significance for
 the microbial community, Harmful Algae, 4, 875-893, 2005.
 817
 818 Brussaard, C. R. D.: Optimization of procedures for counting viruses by flow cytometry, App.
 Environmental Microbiology, 70, 1506-1513, 2003.
 819
 820 Capone, D., Burns, J., Montoya, J., Michaels, A., Subramaniam, A., and Carpenter, E.: New
 821 nitrogen input to the tropical North Atlantic Ocean by nitrogen fixation by the
 cyanobacterium, *Trichodesmium* spp, Global Biogeochemical Cycles, 19, 2004.
 822
 823 Capone, D. G., and Carpenter, E. J.: Nitrogen fixation in the marine environment, Science,
 217, 1140-1142, 1982.
 824
 825 Capone, D. G., Zehr, J. P., Paerl, H. W., Bergman, B., and Carpenter, E. J.: *Trichodesmium*, a
 globally significant marine cyanobacterium, Science, 276, 1221-1229, 1997.
 826
 827 Capone, D. G., Subramaniam, A., Montoya, J. P., Voss, M., Humborg, C., Johansen, A. M.,
 828 Siefert, R. L., and Carpenter, E. J.: An extensive bloom of the N₂-fixing cyanobacterium
 829 *Trichodesmium erythraeum* in the central Arabian Sea, Marine Ecology Progress Series, 172,
 281-292, 1998.
 830
 831 Castruita, M., Saito, M., Schottel, P., Elmegreen, L., Myneni, S., Stiefel, E., and Morel, F. M.:
 832 Overexpression and characterization of an iron storage and DNA-binding Dps protein from
Trichodesmium erythraeum, Applied and Environmental Microbiology, 72, 2918-2924, 2006.
 833
 834 Chappell, P. D., and Webb, E. A.: A molecular assessment of the iron stress response in the
 835 two phylogenetic clades of *Trichodesmium*, Environmental Microbiology, 12, 13-27,
 10.1111/j.1462-2920.2009.02026.x, 2010.
 836
 837 Coleman, M. L., and Chisholm, S. W.: Ecosystem-specific selection pressures revealed
 838 through comparative population genomics, Proceedings of the National Academy of Sciences,
 107, 18634-18639, 2010.
 839
 840 Dandonneau, Y., and Gohin, F.: Meridional and seasonal variations of the sea surface
 841 chlorophyll concentration in the southwestern tropical Pacific (14 to 32 S, 160 to 175 E), Deep
 Sea Research Part A. Oceanographic Research Papers, 31, 1377-1393, 1984.
 842
 843 Dowd, S. E., Callaway, T. R., Wolcott, R. D., Sun, Y., McKeehan, T., Hagevoort, R. G., and
 844 Edrington, T. S.: Evaluation of the bacterial diversity in the feces of cattle using 16S rDNA
 845 bacterial tag-encoded FLX amplicon pyrosequencing (bTEFAP), BMC microbiology, 8, 125,
 2008.

846 Dupouy, C., Benielli-Gary, D., Neveux, J., Dandonneau, Y., and Westberry, T. K.: An
847 algorithm for detecting *Trichodesmium* surface blooms in the South Western Tropical Pacific,
848 Biogeosciences, 8, 3631-3647, 10.5194/bg-8-3631-2011, 2011.

849 Dyhrman, S. T., Chappell, P. D., Haley, S. T., Moffett, J. W., Orchard, E. D., Waterbury, J. B.,
850 and Webb, E. A.: Phosphonate utilization by the globally important marine diazotroph
851 *Trichodesmium*, Nature, 439, 68-71, 2006.

852 Edgar, R. C.: UPARSE: highly accurate OTU sequences from microbial amplicon reads,
853 Nature Methods, 10, 996-998, 2013.

854 Engel, A.: The role of transparent exopolymer particles (TEP) in the increase in apparent
855 particle stickiness (alpha) during the decline of a diatom bloom, Journal of Plankton Research,
856 22, 485-497, 2000.

857 Evans, C., Malin, G., Mills, G. P., and Wilson, W. H.: Viral infection of *Emiliania huxleyi*
858 (prymnesiophyceae) leads to elevated production of reactive oxygen species, Journal of
859 Phycology, 42, 1040-1047, 2006.

860 Frydenborg, B. R., Krediet, C. J., Teplitski, M., and Ritchie, K. B.: Temperature-dependent
861 inhibition of opportunistic vibrio pathogens by native coral commensal bacteria, Microbial
862 Ecology, 67, 392-401, 2014.

863 Georgiou, T., Yu, Y.-T., Ekunwe, S., Buttner, M., Zuurmond, A.-M., Kraal, B., Kleanthous,
864 C., and Snyder, L.: Specific peptide-activated proteolytic cleavage of *Escherichia coli*
865 elongation factor Tu, Proceedings of the National Academy of Sciences, 95, 2891-2895, 1998.

866 Guo, C., and Tester, P. A.: Toxic effect of the bloom-forming *Trichodesmium* sp.
867 (Cyanophyta) to the copepod *Acartia tonsa*, Natural Toxins, 2, 222-227, 1994.

868 Hamady, M., Walker, J. J., Harris, J. K., Gold, N. J., and Knight, R.: Error-correcting
869 barcoded primers for pyrosequencing hundreds of samples in multiplex, Nature Methods, 5,
870 235-237, 2008.

871 Havaux, M., Guedeney, G., Hagemann, M., Yermenko, N., Matthijs, H. C., and Jeanjean, R.:
872 The chlorophyll-binding protein IsiA is inducible by high light and protects the
873 cyanobacterium *Synechocystis* PCC6803 from photooxidative stress, FEBS Letters, 579,
874 2289-2293, 2005.

875 Herbland, A., Le Bouteiller, A., and Raimbault, P.: Size structure of phytoplankton biomass in
876 the equatorial Atlantic Ocean, Deep Sea Research Part A. Oceanographic Research Papers, 32,
877 819-836, 1985.

878 Hewson, I., Govil, S. R., Capone, D. G., Carpenter, E. J., and Fuhrman, J. A.: Evidence of
879 *Trichodesmium* viral lysis and potential significance for biogeochemical cycling in the
880 oligotrophic ocean, Aquatic Microbial Ecology, 36, 1-8, 2004.

881 Hewson, I., Poretsky, R. S., Dyhrman, S. T., Zielinski, B., White, A. E., Tripp, H. J., Montoya,
882 J. P., and Zehr, J. P.: Microbial community gene expression within colonies of the diazotroph,
883 *Trichodesmium*, from the Southwest Pacific Ocean, ISME Journal, 3, 1286-1300,
884 10.1038/ismej.2009.75, 2009.

885 Hmelo, L. R., Van Mooy, B. A. S., and Mincer, T. J.: Characterization of bacterial epibionts
886 on the cyanobacterium *Trichodesmium*, *Aquatic Microbial Ecology*, 67, 1-U119,
887 10.3354/ame01571, 2012.

888 Holmes, R. M., Aminot, A., K  rouel, R., Hooker, B. A., and Peterson, B. J.: A simple and
889 precise method for measuring ammonium in marine and freshwater ecosystems, *Canadian*
890 *Journal of Fisheries and Aquatic Sciences*, 56, 1801-1808, 10.1139/f99-128, 1999.

891 Hove-Jensen, B., Zechel, D. L., and Jochimsen, B.: Utilization of Glyphosate as Phosphate
892 Source: Biochemistry and Genetics of Bacterial Carbon-Phosphorus Lyase, *Microbiology and*
893 *Molecular Biology Reviews*, 78, 176-197, 2014.

894 Hunt, B. P. V., Bonnet, S., Berthelot, H., Conroy, B. J., Foster, R., and Pagano, M.:
895 Contribution and pathways of diazotroph derived nitrogen to zooplankton during the VAHINE
896 mesocosm experiment in the oligotrophic New Caledonia lagoon, *Biogeosciences*
897 *Discussions*, doi:10.5194/bg-2015-614, 2016.

898 Ivars-Martinez, E., Martin-Cuadrado, A.-B., D'Auria, G., Mira, A., Ferriera, S., Johnson, J.,
899 Friedman, R., and Rodriguez-Valera, F.: Comparative genomics of two ecotypes of the marine
900 planktonic copiotroph *Alteromonas macleodii* suggests alternative lifestyles associated with
901 different kinds of particulate organic matter, *The ISME Journal*, 2, 1194-1212, 2008.

902 Jacquet, S., Heldal, M., Iglesias-Rodriguez, D., Larsen, A., Wilson, W., and Bratbak, G.: Flow
903 cytometric analysis of an *Emiliana huxleyi* bloom terminated by viral infection, *Aquatic*
904 *Microbial Ecology*, 27, 111-124, 2002.

905 Jacquet, S., Delesalle, B., Torr  ton, J.-P., and Blanchot, J.: Response of phytoplankton
906 communities to increased anthropogenic influences (southwestern lagoon, New Caledonia),
907 *Marine Ecology Progress Series*, 320, 65-78, 2006.

908 Jeanjean, R., Zuther, E., Yermenko, N., Havaux, M., Matthijs, H. C., and Hagemann, M.: A
909 photosystem 1 *psaFJ*-null mutant of the cyanobacterium *Synechocystis* PCC 6803 expresses
910 the *isiAB* operon under iron replete conditions, *FEBS letters*, 549, 52-56, 2003.

911 Kerbrat, A.-S., Darius, H. T., Pauillac, S., Chinain, M., and Laurent, D.: Detection of
912 ciguatoxin-like and paralysing toxins in *Trichodesmium* spp. from New Caledonia lagoon,
913 *Marine Pollution Bulletin*, 61, 360-366, 2010.

914 Kopylova, E., No  , L., and Touzet, H.: SortMeRNA: fast and accurate filtering of ribosomal
915 RNAs in metatranscriptomic data, *Bioinformatics*, 28, 3211-3217, 2012.

916 Langmead, B., and Salzberg, S. L.: Fast gapped-read alignment with Bowtie 2, *Nature*
917 *Methods*, 9, 357-359, 2012.

918 Latifi, A., Jeanjean, R., Lemeille, S., Havaux, M., and Zhang, C.-C.: Iron starvation leads to
919 oxidative stress in *Anabaena* sp. strain PCC 7120, *Journal of Bacteriology*, 187, 6596-6598,
920 2005.

921 Laudenbach, D. E., and Straus, N. A.: Characterization of a cyanobacterial iron stress-induced
922 gene similar to *psbC*, *Journal of Bacteriology*, 170, 5018-5026, 1988.

923 Leblanc, K., Cornet, V., Caffin, M., Rodier, M., Desnues, A., Berthelot, H., Turk-Kubo, K.,
924 and Heliou, J.: Phytoplankton community structure in the VAHINE mesocosm experiment,
925 Biogeosciences Discussions., doi:10.5194/bg-2015-605, 2016.

926 Lehahn, Y., Koren, I., Schatz, D., Frada, M., Sheyn, U., Boss, E., Efrati, S., Rudich, Y.,
927 Trainic, M., and Sharoni, S.: Decoupling physical from biological processes to assess the
928 impact of viruses on a mesoscale algal bloom, *Current Biology*, 24, 2041-2046, 2014.

929 Luo, Y.-W., Doney, S., Anderson, L., Benavides, M., Berman-Frank, I., Bode, A., Bonnet, S.,
930 Boström, K., Böttjer, D., and Capone, D.: Database of diazotrophs in global ocean:
931 abundance, biomass and nitrogen fixation rates, *Earth System Science Data*, 4, 47-73, 2012.

932 Mackey, K. R., Post, A. F., McIlvin, M. R., Cutter, G. A., John, S. G., and Saito, M. A.:
933 Divergent responses of Atlantic coastal and oceanic *Synechococcus* to iron limitation,
934 *Proceedings of the National Academy of Sciences*, 112, 9944-9949, 2015.

935 Martin, M.: Cutadapt removes adapter sequences from high-throughput sequencing reads,
936 *EMBnet. Journal*, 17, pp. 10-12, 2011.

937 Martinez, A., Tyson, G. W., and DeLong, E. F.: Widespread known and novel phosphonate
938 utilization pathways in marine bacteria revealed by functional screening and metagenomic
939 analyses, *Environmental Microbiology*, 12, 222-238, 10.1111/j.1462-2920.2009.02062.x,
940 2010.

941 Martínez, A., Osburne, M. S., Sharma, A. K., DeLong, E. F., and Chisholm, S. W.: Phosphite
942 utilization by the marine picocyanobacterium *Prochlorococcus* MIT9301, *Environmental*
943 *Microbiology*, 14, 1363-1377, 2012.

944 Massana, R., Murray, A. E., Preston, C. M., and DeLong, E. F.: Vertical distribution and
945 phylogenetic characterization of marine planktonic Archaea in the Santa Barbara Channel,
946 *Applied and Environmental Microbiology*, 63, 50-56, 1997.

947 Michel, K. P., and Pistorius, E. K.: Adaptation of the photosynthetic electron transport chain
948 in cyanobacteria to iron deficiency: the function of IdiA and IsiA, *Physiologia Plantarum*, 120,
949 36-50, 2004.

950 Mohr, W., Grosskopf, T., Wallace, D. W., and LaRoche, J.: Methodological underestimation
951 of oceanic nitrogen fixation rates, *PLOS One*, 5, e12583, 2010.

952 Montoya, J. P., Voss, M., Kahler, P., and Capone, D. G.: A simple, high-precision, high-
953 sensitivity tracer assay for N₂ fixation, *Applied and Environmental Microbiology*, 62, 986-
954 993, 1996.

955 Mulholland, M. R.: The fate of nitrogen fixed by diazotrophs in the ocean, *Biogeosciences*, 4,
956 37-51, 2007.

957 O'Neil, J. M., and Roman, M. R.: Ingestion of the Cyanobacterium *Trichodesmium* spp by
958 Pelagic Harpacticoid Copepods *Macrosetella*, *Miracia* and *Oculostella*, *Hydrobiologia*, 293,
959 235-240, 1994.

- 960 O'Neil, J. M.: The colonial cyanobacterium *Trichodesmium* as a physical and nutritional
961 substrate for the harpacticoid copepod *Macrosetella gracilis*, *Journal of Plankton Research*,
962 20, 43-59, 1998.
- 963 Ohki, K.: A possible role of temperate phage in the regulation of *Trichodesmium* biomass,
964 *Bulletin de l'institute oceanographique, Monaco*, 19, 287-291, 1999.
- 965 Orchard, E., Webb, E., and Dyhrman, S.: Characterization of phosphorus-regulated genes in
966 *Trichodesmium* spp., *The Biological Bulletin*, 205, 230-231, 2003.
- 967 Paerl, H. W., Priscu, J. C., and Brawner, D. L.: Immunochemical localization of nitrogenase in
968 marine *Trichodesmium* aggregates: Relationship to N₂ fixation potential, *Applied and*
969 *Environmental Microbiology*, 55, 2965-2975, 1989.
- 970 Passow, U., and Alldredge, A. L.: A dye binding assay for the spectrophotometric
971 measurement of transparent exopolymer particles (TEP), *Limnology and Oceanography*, 40,
972 1326-1335, 1995.
- 973 Pfreundt, U., Kopf, M., Belkin, N., Berman-Frank, I., and Hess, W. R.: The primary
974 transcriptome of the marine diazotroph *Trichodesmium erythraeum* IMS101, *Scientific*
975 *Reports*, 4, 2014.
- 976 Pfreundt, U., Van Wambeke, F., Caffin, M., Bonnet, S., and Hess, W. R.: Succession within
977 the prokaryotic communities during the VAHINE mesocosms experiment in the New
978 Caledonia lagoon, *Biogeosciences*, 13, 2319-2337, doi:10.5194/bg-13-2319-2016, 2016.
- 979 Pichon, D., Cudennec, B., Huchette, S., Djediat, C., Renault, T., Paillard, C., and Auzoux-
980 Bordenave, S.: Characterization of abalone *Haliotis tuberculata*–*Vibrio harveyi* interactions in
981 gill primary cultures, *Cytotechnology*, 65, 759-772, 2013.
- 982 Pinto, F. L., Thapper, A., Sontheim, W., and Lindblad, P.: Analysis of current and alternative
983 phenol based RNA extraction methodologies for cyanobacteria, *BMC Molecular Biology*, 10,
984 1, 2009.
- 985 Polyviou, D., Hitchcock, A., Baylay, A. J., Moore, C. M., and Bibby, T. S.: Phosphite
986 utilization by the globally important marine diazotroph *Trichodesmium*, *Environmental*
987 *Microbiology Reports*, 7, 824-830, 2015.
- 988 Pujo-Pay, M., and Raimbault, P.: Improvement of the wet-oxidation procedure for
989 simultaneous determination of particulate organic nitrogen and phosphorus collected on filters,
990 *Marine Ecology-Progress Series*, 105, 203–207, 10.3354/meps105203, 1994.
- 991 Quast, C., Pruesse, E., Yilmaz, P., Gerken, J., Schweer, T., Yarza, P., Peplies, J., and
992 Glöckner, F. O.: The SILVA ribosomal RNA gene database project: improved data processing
993 and web-based tools, *Nucleic Acids Research*, 41, D590-D596, 10.1093/nar/gks1219, 2013.
- 994 Rahav, E., Herut, B., Levi, A., Mulholland, M., and Berman-Frank, I.: Springtime contribution
995 of dinitrogen fixation to primary production across the Mediterranean Sea, *Ocean Science*, 9,
996 489-498, 2013.
- 997 Rodier, M., and Le Borgne, R.: Population dynamics and environmental conditions affecting
998 *Trichodesmium* spp. (filamentous cyanobacteria) blooms in the south-west lagoon of New

999 Caledonia, Journal of Experimental Marine Biology and Ecology, 358, 20-32,
1000 10.1016/j.jembe.2008.01.016, 2008.

1001 Rodier, M., and Le Borgne, R.: Population and trophic dynamics of *Trichodesmium thiebautii*
1002 in the SE lagoon of New Caledonia. Comparison with *T. erythraeum* in the SW lagoon,
1003 Marine Pollution Bulletin, 61, 349-359, 2010.

1004 Shaked, Y.: Iron redox dynamics and biogeochemical cycling in the epilimnion of Lake
1005 Kinneret, PhD thesis, Hebrew University of Jerusalem, 2002.

1006 Sheridan, C. C., Steinberg, D. K., and Kling, G. W.: The microbial and metazoan community
1007 associated with colonies of *Trichodesmium* spp.: a quantitative survey, Journal of Plankton
1008 Research, 24, 913-922, 2002.

1009 Siddiqui, P. J., Bergman, B., Bjorkman, P. O., and Carpenter, E. J.: Ultrastructural and
1010 chemical assessment of poly-beta-hydroxybutyric acid in the marine cyanobacterium
1011 *Trichodesmium thiebautii*, FEMS Microbiology Letters, 73, 143-148, 1992.

1012 Smetacek, V.: Role of sinking in diatom life-history cycles: ecological, evolutionary and
1013 geological significance, Marine Biology, 84, 239-251, 1985.

1014 Snow, J. T., Polyviou, D., Skipp, P., Christmas, N. A., Hitchcock, A., Geider, R., Moore, C.
1015 M., and Bibby, T. S.: Quantifying Integrated Proteomic Responses to Iron Stress in the
1016 Globally Important Marine Diazotroph *Trichodesmium*, PLOS One, 10, e0142626, 2015.

1017 Spungin, D., Berman-Frank, I., and Levitan, O.: *Trichodesmium's* strategies to alleviate
1018 phosphorus limitation in the future acidified oceans, Environmental Microbiology, 16, 1935-
1019 1947, 2014.

1020 Spungin, D., Rosenberg, G., Bidle, K. D., and Berman-Frank, I.: Metacaspases and bloom
1021 demise in the marine cyanobacterium *Trichodesmium*, In Prep.

1022 Strickland, J. D. H., and Parsons, T. R.: A Practical Handbook of Seawater Analysis, Fisheries
1023 Research Board of Canada, Ottawa, 1972.

1024 Tandeau de Marsac, N., and Houmard, J.: Complementary chromatic adaptation:
1025 Physiological conditions and action spectra, in: Methods in Enzymology, Academic Press,
1026 318-328, 1988.

1027 Tarutani, K., Nagasaki, K., and Yamaguchi, M.: Viral impacts on total abundance and clonal
1028 composition of the harmful bloom-forming phytoplankton heterosigma akashiwo, Applied and
1029 Environmental Microbiology, 66, 4916-4920, 2000.

1030 Thamatrakoln, K., Korenovska, O., Niheu, A. K., and Bidle, K. D.: Whole-genome expression
1031 analysis reveals a role for death-related genes in stress acclimation of the diatom *Thalassiosira*
1032 *pseudonana*, Environmental Microbiology, 14, 67-81, 2012.

1033 Turk-Kubo, K., Frank, I., Hogan, M., Desnues, A., Bonnet, S., and Zehr, J.: Diazotroph
1034 community succession during the VAHINE mesocosms experiment (New Caledonia Lagoon),
1035 Biogeosciences 12, 7435-7452, doi:10.5194/bg-12-7435-2015, 2015.

- Van Mooy, B. A., Hmelo, L. R., Sofen, L. E., Campagna, S. R., May, A. L., Dyhrman, S. T., Heithoff, A., Webb, E. A., Momper, L., and Mincer, T. J.: Quorum sensing control of phosphorus acquisition in *Trichodesmium* consortia, *The ISME Journal*, 6, 422-429, 2012.
- Van Wambeke, F., Pfreundt, U., Barani, A., Berthelot, H., Moutin, T., Rodier, M., Hess, W. R., and Bonnet, S.: Heterotrophic bacterial production and metabolic balance during the VAHINE mesocosm experiment in the New Caledonia lagoon, *Biogeosciences Discussions*, 12, 19861-19900, doi:10.5194/bgd-12-19861-2015, 2015.
- Vardi, A., Berman-Frank, I., Rozenberg, T., Hadas, O., Kaplan, A., and Levine, A.: Programmed cell death of the dinoflagellate *Peridinium gatunense* is mediated by CO₂ limitation and oxidative stress, *Current Biology: CB*, 9, 1061-1064, 1999.
- Vardi, A., Haramaty, L., Van Mooy, B. A., Fredricks, H. F., Kimmance, S. A., Larsen, A., and Bidle, K. D.: Host-virus dynamics and subcellular controls of cell fate in a natural coccolithophore population, *Proceedings of the National Academy of Sciences*, 109, 19327-19332, 2012.
- Walsby, A. F.: The properties and bouyancy providing role of gas vacuoles in *Trichodesmium*, *British Phycological Journal*, 13, 103-116, 1978.
- Weitz, J. S., and Wilhelm, S. W.: Ocean viruses and their effects on microbial communities and biogeochemical cycles, *F1000 Biology Reports*, 4, 17, 2012.
- Wu, Z., Jenkins, B. D., Rynearson, T. A., Dyhrman, S. T., Saito, M. A., Mercier, M., and Whitney, L. P.: Empirical bayes analysis of sequencing-based transcriptional profiling without replicates, *BMC Bioinformatics*, 11, 564, 2010.
- Zehr, J. P.: Nitrogen fixation in the Sea: Why Only *Trichodesmium*, in: *Molecular Ecology of Aquatic Microbes*, edited by: Joint, I., NATO ASI Series, Springer-Verlag, Heidelberg, 335-363, 1995.

Figure legends

Figure 1. Temporal dynamics of pre-bloom measurements in the lagoon waters (a) Chl *a* concentrations ($\mu\text{g L}^{-1}$), (b) Virus like particles (VLP, $\text{mL}^{-1} \times 10^6$), (c) N₂ fixation rates ($\text{nmol L}^{-1} \text{h}^{-1}$) and particulate organic nitrogen (PON, $\mu\text{mol L}^{-1}$). (d) Changes in the concentrations of transparent exopolymeric particles (TEP, $\mu\text{g GX L}^{-1}$) and particulate organic carbon (POC, $\mu\text{mol L}^{-1}$). Water was sampled from in the lagoon outside the VAHINE mesocosms, at 1 m depth (surface) throughout the experimental period from day 2 to 23 (n=3). For VLP, the standard error for technical replicates (n=3) was < 1 %, which is smaller than symbol size.

Figure 2. (a-c) Dense surface blooms of *Trichodesmium* observed outside the mesocosms in the lagoon waters on day 23 at 12:00. Photos illustrate the spatial heterogeneity of the surface accumulations and the high density of the biomass. (d-e) To examine the mechanistic of demise (Experiment 1), *Trichodesmium* filaments and colonies were collected by plankton net (mesh size, 80 μm) from the dense surface bloom (day 23, 12:00 h; designated T_0) and resuspended in 0.2 μm pore-size filtered seawater (FSW) in six 4.5 L bottles. Bottles were incubated on-deck in running-seawater pools with ambient surface temperature ($\sim 26^\circ\text{C}$) at 50 % of the surface irradiance. Bottles were sampled every 2-4 h for different parameters until the biomass crashed. (f) Temporal changes in Chl *a* concentrations in the bottles from the time of biomass collection and resuspension in the bottles until the *Trichodesmium* biomass crashed ~ 24 h after the experiment began ($n=3-6$). Photo c. courtesy of A. Renaud.

Figure 3. Dynamics of microbial community abundance and diversity during *Trichodesmium* surface bloom as obtained by 16S rRNA gene sequencing for samples collected from the surface waters outside the mesocosms during *Trichodesmium* surface accumulation (bloom) (short-term experiment 1). Pie charts show the changes in dominant groups during the *Trichodesmium* bloom and crash from two replicate incubation bottles (please note, *Oscillatoriales* consisted only of *Trichodesmium* in this experiment). The graphs below show the respective temporal dynamics of *Trichodesmium* (gray circles) and *Alteromonas* (white triangles), the dominant bacterial species during the incubation experiment.

Figure 4. Short-term experiment 2 - measurements from the lagoon waters following *Trichodesmium* bloom on day 23. (a) Virus like particles (VLP, $\text{mL}^{-1} \times 10^6$) and *Trichodesmium* abundance (trichomes L^{-1}) derived from qPCR-based abundances of *Trichodesmium nifH* gene copies (Bonnet et al. 2016b) based on the assumption of 100 gene-copies per trichome (b) N_2 fixation rates ($\text{nmol L}^{-1} \text{h}^{-1}$), particulate organic nitrogen (PON, $\mu\text{mol L}^{-1}$) and ammonium concentrations (NH_4^+ , $\mu\text{mol L}^{-1}$). (c) Changes in the concentrations of transparent exopolymeric particles (TEP, $\mu\text{g GX L}^{-1}$) and particulate organic carbon (POC, $\mu\text{mol L}^{-1}$). For experiment 2, seawater from the surface bloom was collected 5 h after the initial surface bloom was sighted (day 23, 17:00) by directly filling 20 L polyethylene carboys gently to avoid destroying biomass. Bottles were placed in on-deck incubators filled with running seawater to maintain ambient surface temperature ($\sim 26^\circ\text{C}$) and covered with neutral screening at 50 % surface irradiance levels. For all parameters, replicates were $n=3$. For VLP, the standard error for technical replicates ($n=3$) was $< 1\%$, which is smaller than symbol size.

Figure 5. (a) Expression of alkaline phosphatase associated genes *phoA* and *phoX* (Tery_3467 and Tery_3845), phosphite utilization genes *ptxA*, *ptxB* and *ptxC* (Tery_0365- Tery_0367), and phosphonate utilization genes (*phn* genes, Tery_4993, Tery_4994, Tery_4995, Tery_4996*, Tery_4997, Tery_4998, Tery_4999, Tery_5000, Tery_5001 Tery_5002 and Tery_5003). Asterisks near locus tag numbers indicate gene duplicates. (b) Iron-related genes, *isiB* (Tery_1666), *isiA* (Tery_1667), *idiA* (Tery_3377), and ferritin DPS gene *dpsA* (Tery_4282). Bars represent log2 fold changes of corresponding genes at T₈ (8 hours after T₀) and T₂₂ (22 hours after T₀) in comparison to T₀. Significant expression was tested with ASC (Wu et al., 2010) and marked with an asterisk. Black asterisks represent significant change from T₀. A gene was called differentially expressed if $P > 0.98$ (posterior probability).

Figure 6. (a) Dynamics of caspase-specific activity rates ($\text{pmol L}^{-1} \text{min}^{-1}$) of *Trichodesmium* in the New Caledonian lagoon during bloom accumulation and bloom demise, sampled during experiment 1. Samples (n=6) collected from the bloom (day 23, 12:00 T₀), were incubated on-deck in an incubator fitted with running seawater to maintain ambient surface temperature (~ 26 °C). (b) Transcript accumulation of metacaspase genes in the *Trichodesmium* bloom during the short-term incubation experiment. Metacaspase genes are *TeMC1* (Tery_2077), *TeMC2* (Tery_2689), *TeMC3* (Tery_3869), *TeMC4* (Tery_2471), *TeMC5* (Tery_2760), *TeMC6* (Tery_2058), *TeMC7* (Tery_1841), *TeMC8* (Tery_0382), *TeMC9* (Tery_4625), *TeMC10* (Tery_2624), *TeMC11* (Tery_2158) and *TeMC12* (Tery_2963). Bars represent log2 fold changes at T₈ (8 hours after T₀) and T₂₂ (22 hours since T₀) in comparison to T₀. Significant expression was tested with ASC (Wu et al., 2010) and marked with an asterisk. Black asterisks represent significant change from T₀. A gene was called differentially expressed if $P > 0.98$ (posterior probability).

Figure 7. Change in gas vesicle protein (*gvp*) genes as obtained from metatranscriptomic analyses of the *Trichodesmium* bloom from peak to collapse (experiment 1). *gvpA* genes (Tery_2330 and Tery_2335*) encode the main constituent of the gas vesicles that forms the essential core of the structure; *gvpN* (Tery_2329 and Tery_2334) *gvpK* (Tery_2322), *gvpG* (Tery_2338) and *gvpL/gvpF* (Tery_2339 and Tery_2340*) encode vesicle synthesis proteins. Bars represent log2 fold changes at T₈ (8 hours after T₀) and T₂₂ (22 hours since T₀) in comparison to T₀. Significant expression was tested with ASC (Wu et al., 2010) and marked with an asterisk. Black asterisks represent significant change from T₀. A gene was called differentially expressed if $P > 0.98$ (posterior probability).

1134

1135

1136

1137

1138

1139

1140

1141

1142

1143

1144

1145

1146

1147

1148

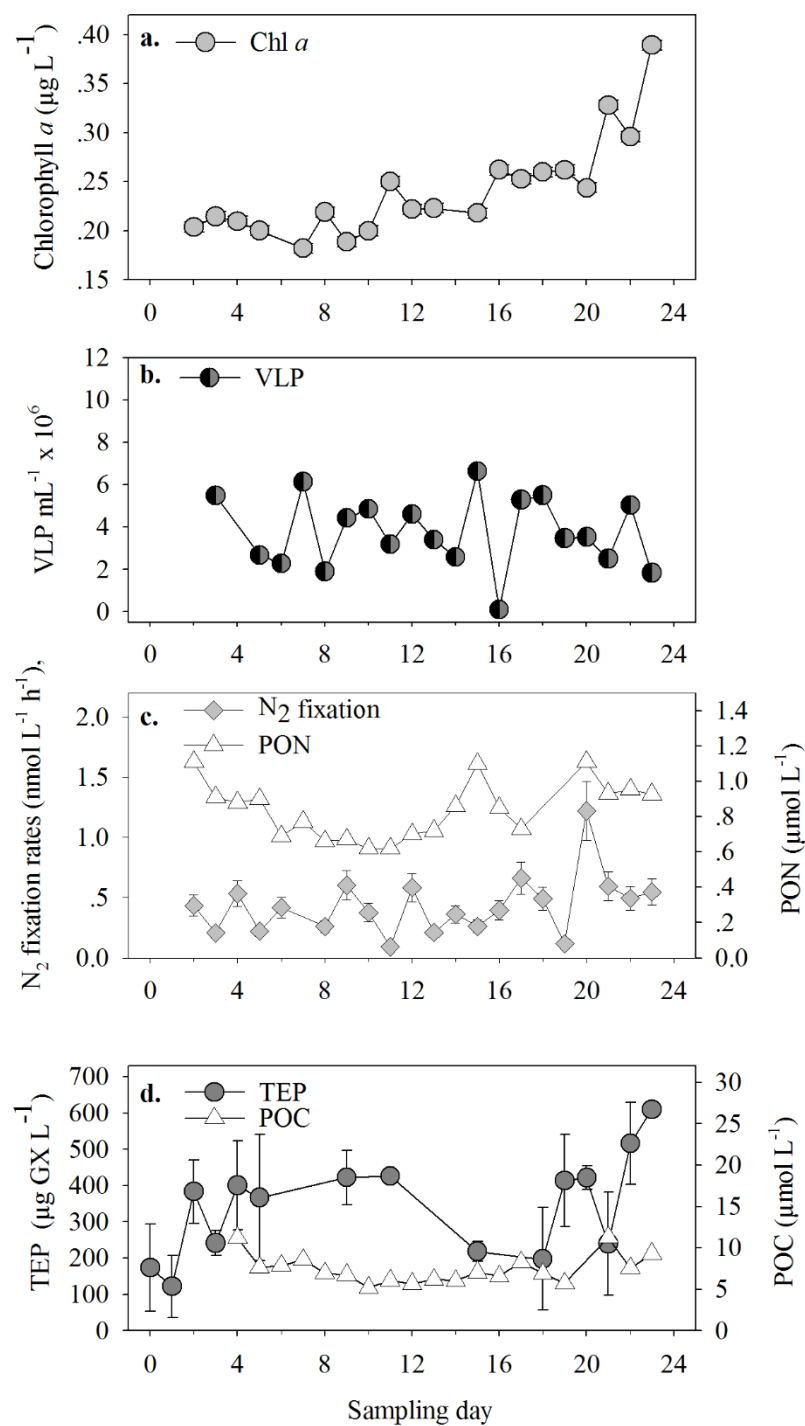
1149

1150

1151

1152

1153 **Figure 1**



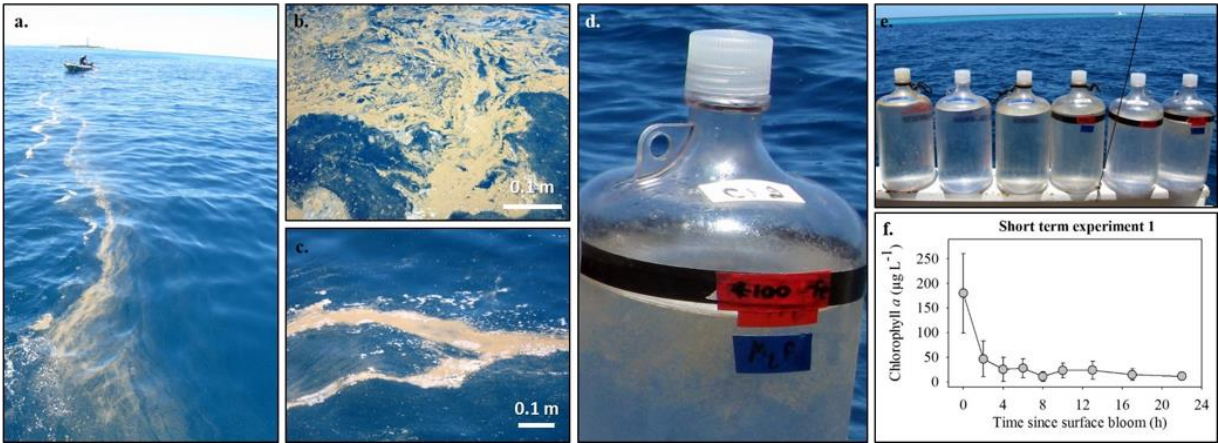
1154

1155

1156

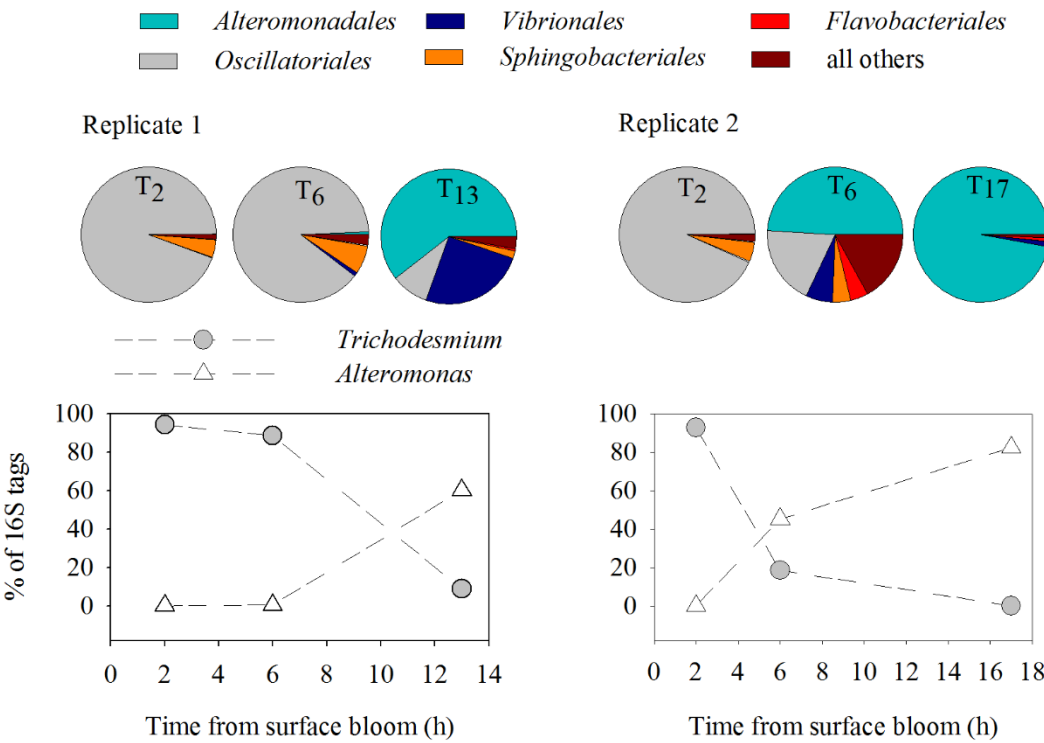
1157

Figure 2



1176

1177 **Figure 3**



1178

1179

1180

1181

1182

1183

1184

1185

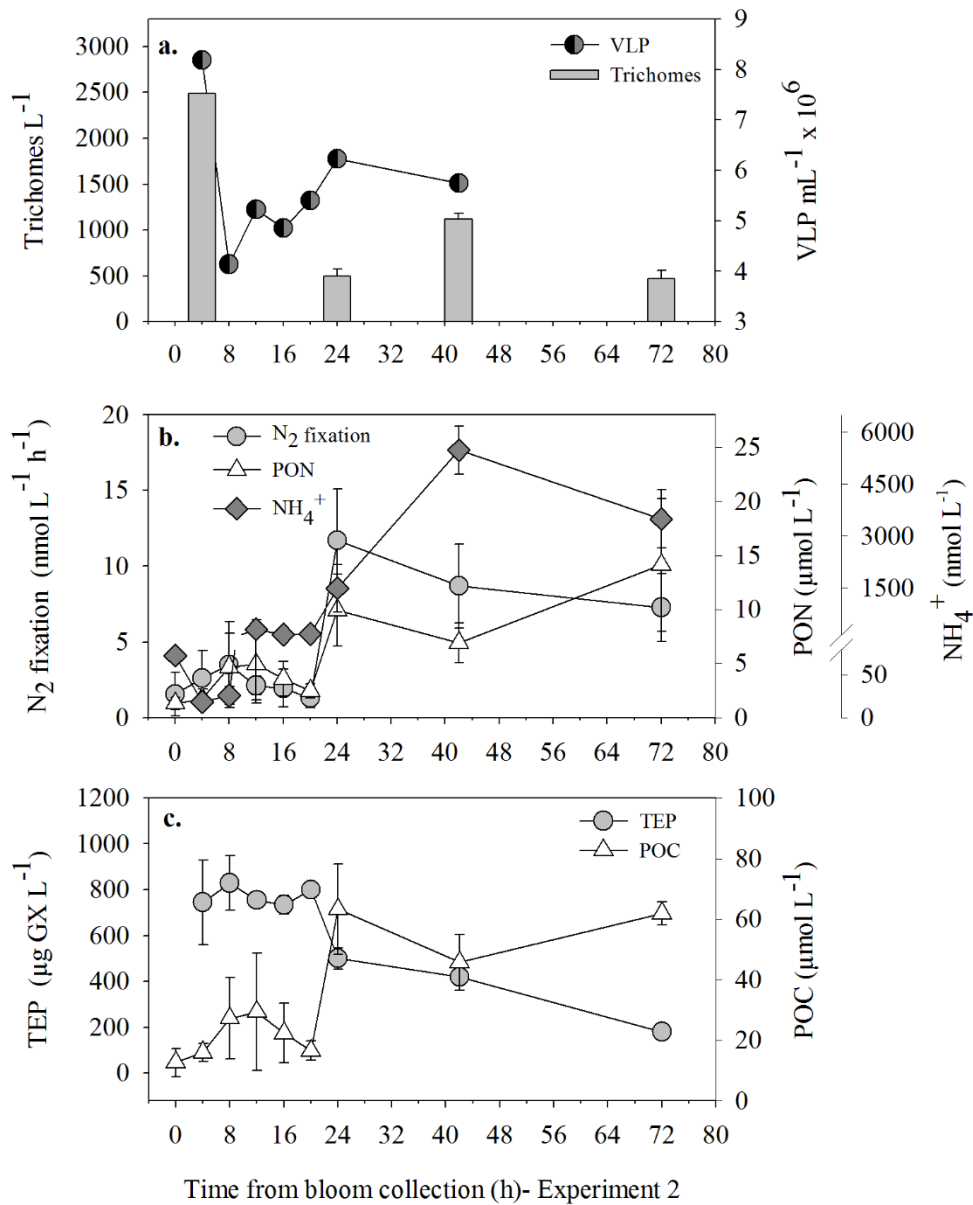
1186

1187

1188

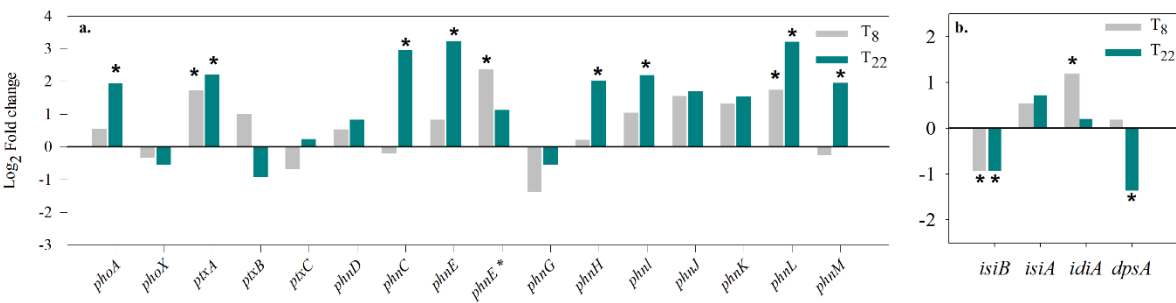
1189

Figure 4



1198

1199 **Figure 5**



1200

1201

1202

1203

1204

1205

1206

1207

1208

1209

1210

1211

1212

1213

1214

Figure 6

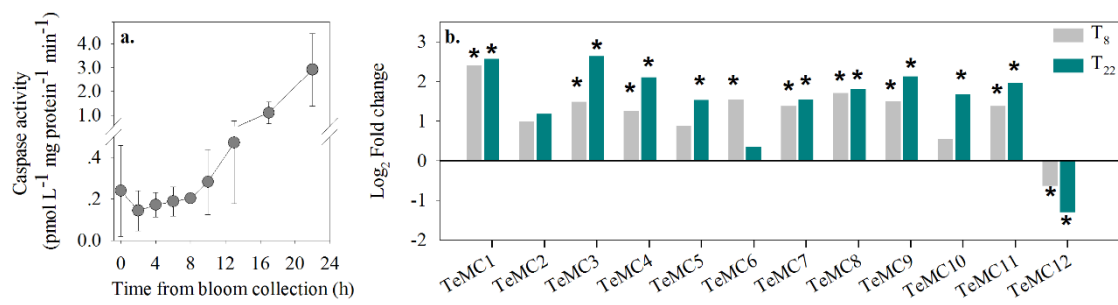


Figure 7

